Electronic Supplementary Information

Table of contents

1. Synthesis

Reaction temperatures refer to the medium that surrounded the reaction vessel. Irradiation and reduction experiments were performed under an argon- or nitrogen-gas atmosphere. Solvents were usually removed under reduced pressure at 40 °C with a rotatory evaporator. The room temperature was approximately 22 °C.

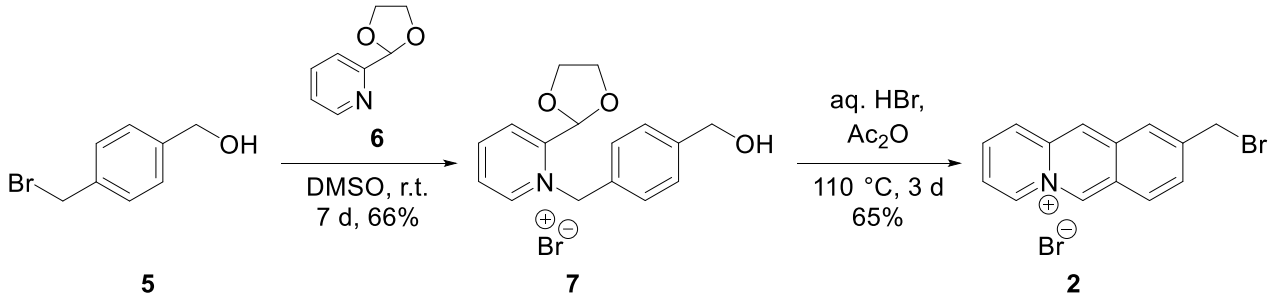

Scheme S1. Cyclodehydration route to 9-(bromomethyl)benzo[*b*]quinolizinium bromide (**2**).

1-(4'-Hydroxymethylbenzyl)-2-(1,3-dioxolan-2-yl)pyridinium bromide (**7**). A suspension of **5** (5.50 g, 27.4 mmol) and **6** (4.14 g, 27.4 mmol) in DMSO (4 mL) was stirred for 6 d under an argon-gas atmosphere at 40 °C. The resulting solution was added dropwise to a solution of ethyl acetate (1.3 L) under vigorous stirring. The resulting precipitate was filtered off and crystallized from ethyl acetate/MeOH to furnish the product as colorless crystals (6.41 g, 66%); mp (145–146 °C). – ^{1}H-NMR (500 MHz, DMSO-d_6): δ = 4.13 (s, 4H, 3''-H, 4''-H), 4.51 (s, 2H, C4'-CH_2), 5.98 (s, 2H, N-CH_2), 6.51 (s, 1H, 1''-H), 7.32 (d, ^{3}J = 8 Hz, 2H, 2'-H, 6'-H), 7.38 (d, ^{3}J = 8 Hz, 2H, 3'-H, 5'-H), 8.20 (ddd, ^{3}J = 8 Hz, ^{3}J = 6 Hz, ^{4}J = 2 Hz, 1H, 5-H), 8.32 (dd, ^{3}J = 8 Hz, ^{4}J = 2 Hz, 1H, 3-H), 8.72 (td, ^{3}J = 8 Hz, ^{4}J = 1 Hz, 1H, 4-H), 9.03 (dd, ^{3}J = 6 Hz, ^{4}J = 1 Hz, 1H, 6-H). – ^{13}C-NMR (125 MHz, DMSO-d_6): δ = 59.8 (N-*C*H_2), 62.3 (C4'-*C*H_2), 65.7 (C3'', C4''), 97.1 (C1''), 126.0 (C3), 127.0 (C3', C5'), 128.2 (C2', C6'), 128.6 (C5), 131.8 (C1'), 143.6 (C4'), 147.1 (C6), 147.1 (C4), 152.0 (C2). – MS (ESI^{+}): *m/z* (%) = 272 (100) [M−Br^{-}]$^{+}$. – El. Anal. for $C_{16}H_{18}BrNO_3$, calcd. (%): C 54.56, H 5.15, N 3.98, found (%): C 54.65, H 5.28, N 4.02.

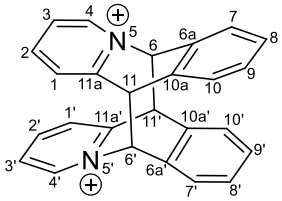

Figure S1. General numbering of the photodimers of benzo[*b*]chinolizinium derivatives.

Comment on the interpretation of ^{1}H-NMR signals of the bridgehead and CH_2 protons of **c1^{shh}** and **c1^{sht}**: The complex coupling pattern (AB, AX) results from a) the diastereotopic methylene protons, b) the reduced conformational flexibility of the methylene units in the cyclomers and b) loss of symmetry because of the strain-induced distortion from the ideal dimer structure by the relatively short linker unit.

2. Reduction reactions

Photometric analysis

To a solution of **1** (*c* = 20 µM) in BPE buffer (pH = 7.80) was added DTT or GSH (*c* = 10 mM) under a nitrogen-gas atmosphere at 20 °C. An absorption spectrum before the addition of the reducing agent and after 3 h at 37 °C was recorded (Figure S2, A1–2). Additionally, a spectrum of the solution of **1** in the presence of GSH was recorded after 16 h at 37 °C (Figure S2, B).

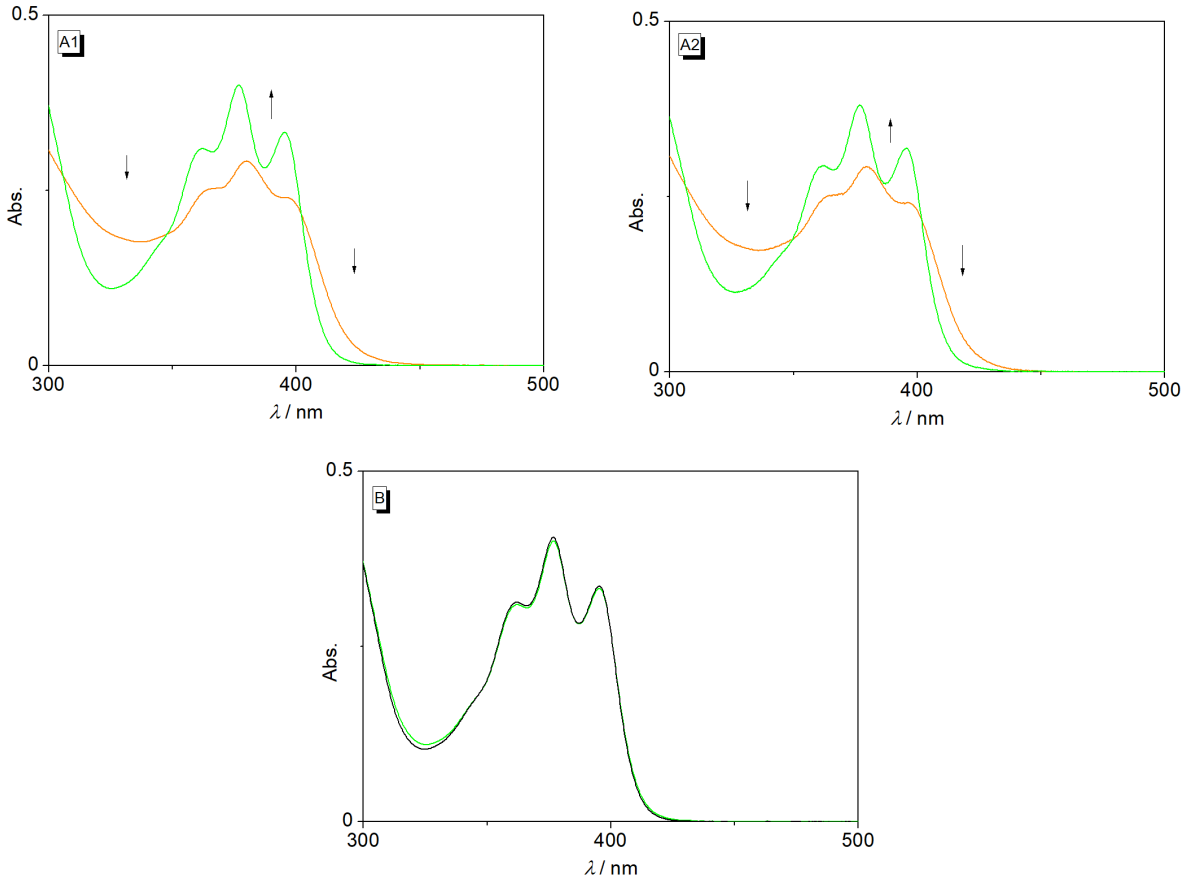

Figure S2. Absorption spectra of **1** (*c* = 20 µM) before (orange) and after treatment with glutathione (GSH, *c* = 10 mM, A1, B) or dithiothreitol (DTT, *c* = 10 mM, A2) for 3 h (green) and after 16 h (B, black) at 37 °C in BPE buffer (pH = 7.80).

NMR-spectroscopic analysis

To further investigate the reaction of **1** in the presence of reducing agents, the experiments were performed on a larger scale under similar conditions, and the reducing process was stopped by the addition of acid. Subsequently, the reaction mixture was extracted, and the extracts were investigated by ^{1}H-NMR-spectroscopic analysis. Because of the fast oxidation to the disulfide **1** in the absence of reducing agents, no further purification steps were conducted.

*General Procedure 1 (GP1) for the reduction of 9,9'-[disulfanediylbis(methylene)]bis benzo[b]chinolizinium bromide (**1**)*

To a solution of **1** (15 mg, 25 µmol) in BPE buffer (pH = 7.9, 50 mL) was added the reducing reagent (*c* = 61.8 mM) under argon-gas atmosphere, and the solution was stirred for 2.5 h at 37 °C. A solution of aq. HPF_6 (60%, 2 mL) was added and the resulting suspension was extracted with CH_2Cl_2 (3 x 50 mL). The combined organic layers were washed with brine (1 x 50 mL) under argon-gas atmosphere and dried with Na_2SO_4. After filtration under argon-gas atmosphere the solvents were removed in vacuo to give the crude product, which was analyzed by ^{1}H-NMR spectroscopy.

Attempt 1:

According to GP1 compound **1** was treated with GSH to give 6 mg of a yellow oil. ^{1}H-NMR-spectroscopic investigations (Figure S3, 2) revealed the presence of a mixture of **1**, **4** and an unidentified side product **8** in a ratio of **1**:**4**:**8** of 48:32:20 (in %).

Attempt 2:

According to GP1 compound **1** was treated with dithiothreitol (DTT) as a reducing agent to give 23 mg of a yellow oil. ^{1}H-NMR-spectroscopic investigations (Figure S3, 3) revealed the presence of a mixture in the ratio of 75% free thiol **4** and 25% of an unidentified side product **9**.

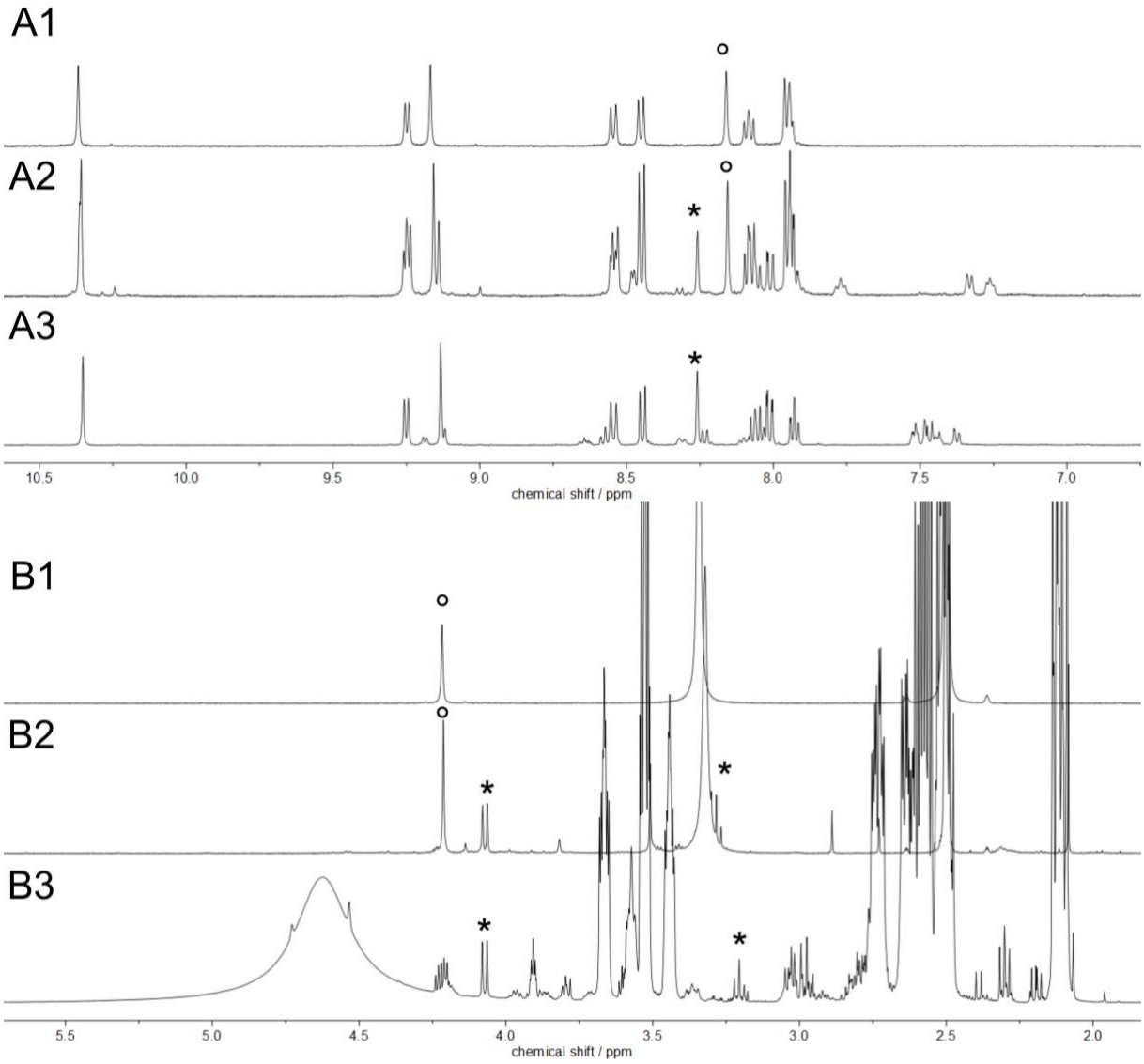

Figure S3. ^{1}H-NMR spectra (DMSO-d_6, 25 °C) (7.0–10.5 ppm, A; 2.0–5.5 ppm, B) of **1** before (1) and after treatment with GSH (2) or DTT (3). ○: Characteristic signals of **1**; ✱: Characteristic signals of **4**.

The ^{1}H-NMR-spectroscopic investigations of the reductions on a larger scale demonstrated that the product **4** has formed in both cases as indicated by the characteristic NMR signals of the sulfanylmethyl substituent, specifically the coupling between the methylene group (^{3}J = 4.02 ppm, 8 Hz) and thiol functionality (t, ^{3}J = 8 Hz). With GSH as a reducing agent, however, 48% of **1** was detected in the ^{1}H NMR spectrum of the product mixture. As GSH is less soluble in dichloromethane and thus no longer available to protect **4** towards oxidation, as indicated by the aliphatic region of the ^{1}H NMR spectrum of the extract, the thiol **4** is presumably oxidized during work up. Furthermore, the experiments in the cuvette (Figure S2, A1 and A2, Figure 2 in main manuscript) indicated that the conversion of **4** to the thiol is essentially the same as with DTT. Another by-product (20% in GSH) and (25% in DTT) was detected in the processed product mixture, that could not be further identified. With the available experimental data, it

remains speculative whether this by-product is also formed under the smaller-scale conditions applied in the cuvette; however, considering the chemical sensitivity of the sulfide functionality we assume that this by-product is formed only under the particular work-up conditions described above.

3. Photocycloaddition reactions

Photometric monitoring of the photoreaction

The photocycloaddition of **1** in PBS solution (pH = 7.80, c = 20 µM, λ_{ex} = 365 nm) was followed photometrically. For comparison, the photoreaction of the parent benzo[*b*]quinolizinium ion **10** (Figure S4) in water (c = 20 µM, λ_{ex} = 365 nm) was also performed and analyzed under otherwise identical conditions (Figure S5). The experiment showed that the reaction of the intermolecular photocycloaddition of **10** is approx. 500 times slower than the intramolecular reaction of **1**.

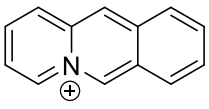

10

Figure S4. Structure of the benzo[*b*]quinolizinium ion (**10**).

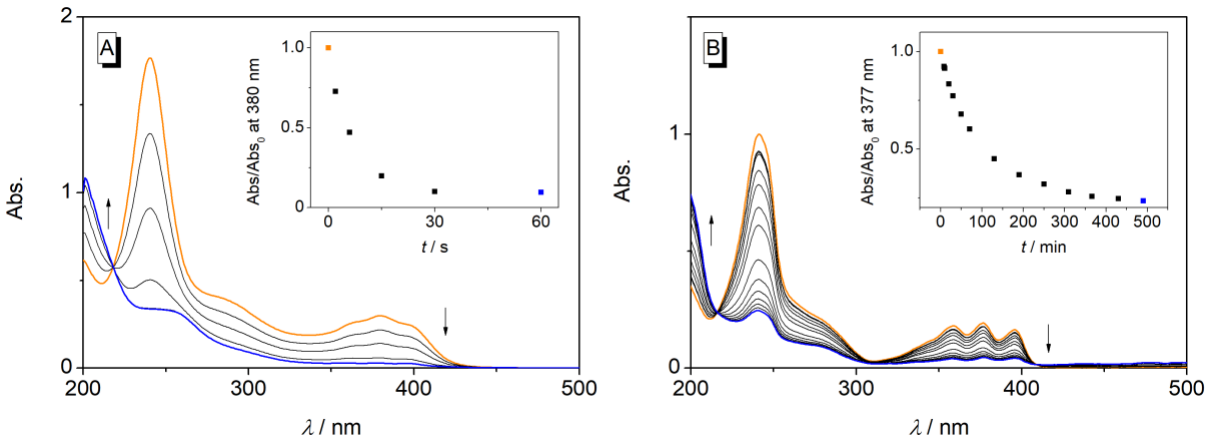

Figure S5. Photometric monitoring of the irradiation (c = 20 µM) of **1** (A, PBS solution, pH 7.80) and **10** (B, water) with λ_{ex} = 365 nm. Inset: Change of absorbance at the absorption maximum during irradiation.

NMR-spectroscopic analysis of the photoreaction

A solution of **1** (12 mg, 20 µmol, 40 µM) in PBS buffer (pH = 7.80, 500 mL) was irradiated at λ_{exc} = 365 nm for 19 min at 20 °C under a nitrogen-gas atmosphere, and the conversion was monitored by absorption spectroscopy. An aqueous solution of HPF_6 (60%, 2 mL) was added dropwise to the resulting photoproducts (250 mL). The solution was extracted with CH_2Cl_2 (3 × 50 mL) and the combined organic layers were washed with brine (1 × 30 mL) and dried with Na_2SO_4. After filtration, the solvent was removed under reduced pressure to give a yellow residue, which was analyzed by ^{1}H-NMR spectroscopy. The product mixture contained the *syn*-head-to-head cycloadduct **c1^{shh}** (70%), the *syn*-head-to-tail product **c1^{sht}** (22%), and the *syn*-head-to-head photodimer **[4]$_2^{shh}$** (8%).

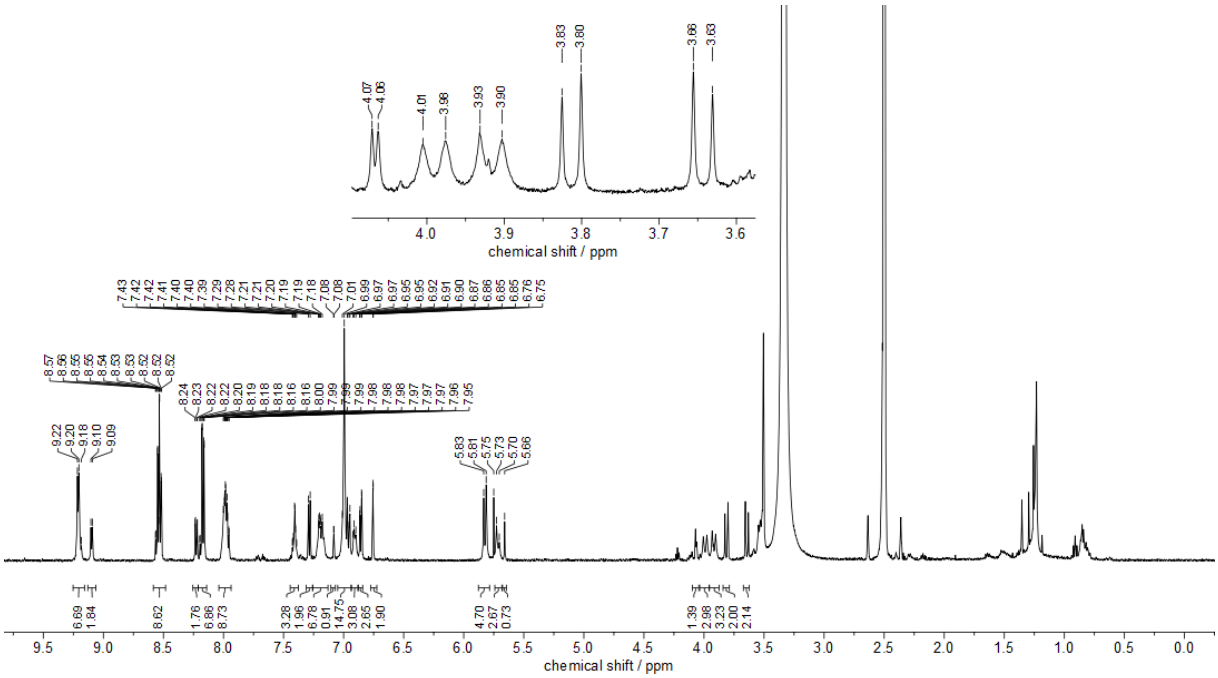

Figure S6. ^{1}H-NMR spectrum (600 MHz, DMSO-d_6, 25 °C) of the photoproducts of **1** (c = 40 µM) after irradiation at λ_{exc} = 365 nm for 19 min and subsequent extraction.

The ^{1}H-NMR-spectroscopic investigations of the photocycloaddition on a larger scale demonstrated that the products **c1^{shh}**, **c1^{sht}** and **[4]$_2^{shh}$** were formed, as indicated by the characteristic ^{1}H-NMR signals of the bridgehead protons at 11-H (5.5–6.0 ppm) and the CH_2-signals (3.0–4.0 ppm). In comparison with the irradiation in the NMR tube, which was performed in D_2O (*cf*. main manuscript) the CH_2-signal in DMSO-d_6 (d, 4.03 ppm, 4 Hz) of the photodimer **[4]$_2^{shh}$** even split up to a doublet that corresponds to the coupling to the thiol functionality, as observed also with an authetic sample of **4**. The isomeric distribution was essentially the same within the error margin as the one obtained at much higher concentrations.

Investigation of the photoreactivity of the photocycloadducts

After completion of the primary photocycloaddition of **1** (1.6 mg, 2.6 µmol, *t* = 13 min) in D_2O (500 µL) the resulting product mixture was irradiated (λ_{ex} = 365 nm) in a NMR tube, and the reaction mixture was analyzed by ^{1}H-NMR spectroscopy after 105 min and 6.5 h of irradiation (Figure S7). The proton signals of the isomer **c1^{shh}** decreased with prolonged irradiation time whereas the proton signals of **[4]$_2^{shh}$** increased, whilst the ones of **c1^{sht}** did not change.

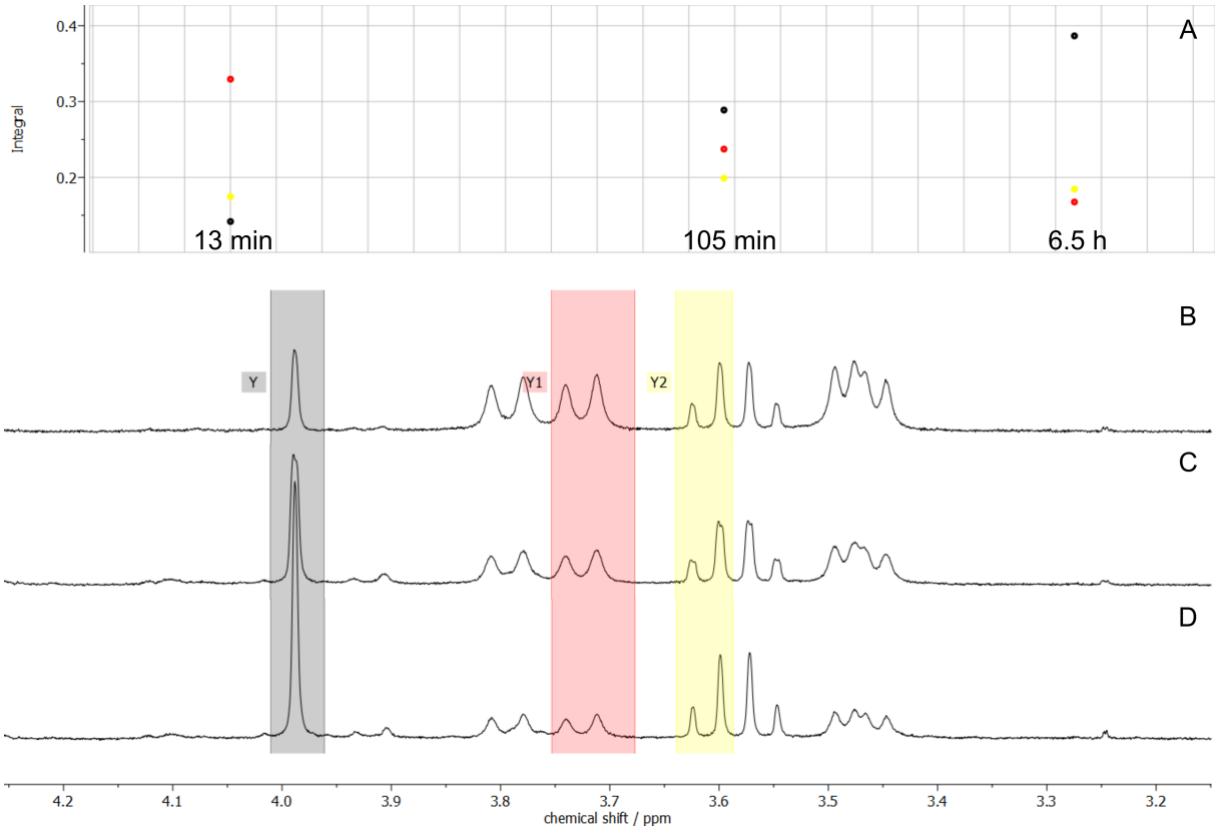

Figure S7. ^{1}H-NMR spectra (D_2O, 25 °C, B–D) (3.2–4.2 ppm) and corresponding integrals graph (A, derived from integrated integrals tool in MestReNova) of **1** after the irradiation of the photoproducts **c1^{shh}** (red), **c1^{sht}** (yellow) and **[4]$_2^{shh}$** (black) (λ_{ex} = 365 nm) for 13 min (B), 105 min (C) and after 6.5 h (D).

4. Investigation of the reactivity of the cycloadducts c1^{shh}, c1^{sht}, and [4]$_2^{shh}$

Photometric monitoring

a) The photocycloadducts **c1^{shh}**, **c1^{sht}**, and **[4]$_2^{shh}$** were heated at *T* = 55 °C for 90 min in PBS solution (pH = 7.80, *c* = 20µM) and the solution was analyzed photometrically (Figure S8A).

b) The photocycloadducts **c1^{shh}**, **c1^{sht}**, and **[4]$_2^{shh}$** were irradiated in PBS solution (pH = 7.80, *c* = 20µM, λ_{ex}= 270 nm) for *t* = 18 min and the reaction was followed photometrically (Figure S8B).

c) The photocycloadducts **c1**^{shh}**, c1**^{sht}**,** and **[4]**$_2^{shh}$ were heated for 5 h at *T* = 37 °C in BPE solution (pH = 7.80, *c* = 20µM) in the presence of DTT (*c* = 10 mM) and the solution was analyzed photometrically (Figure S9).

d) The photocycloadducts **c1**^{shh}**, c1**^{sht}**,** and **[4]**$_2^{shh}$ were heated for 16 h at *T* = 55 °C in PBS solution (pH = 7.80, *c* = 20µM) in the presence of ct DNA (c = 40 µM) and the solution was analyzed photometrically (Figure S10).

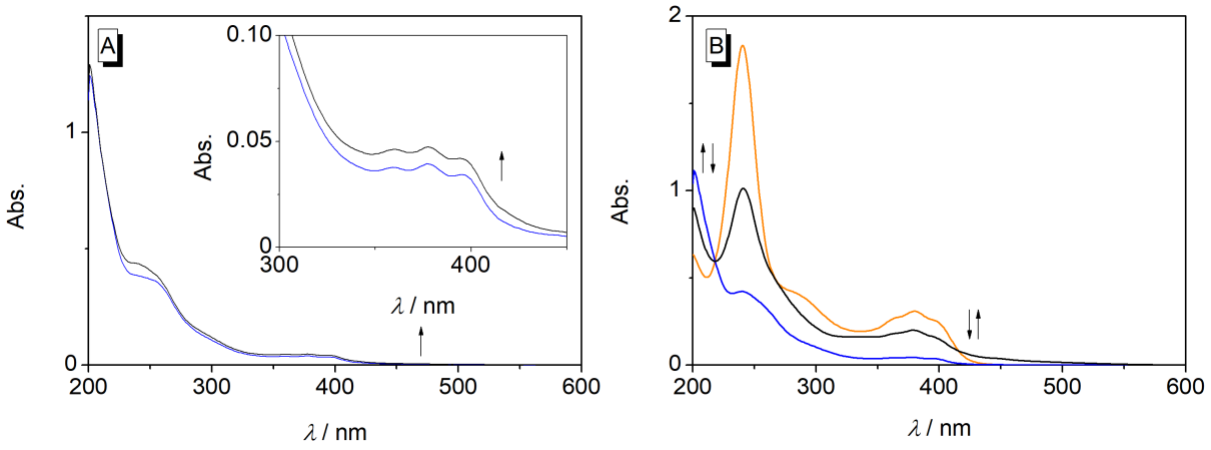

Figure S8. A: Photometric monitoring of thermal treatment of photocylcoadducts **c1**^{shh}, **c1**^{sht}, and **[4]**$_2^{shh}$ (*c* = 20 µM, PBS solution, pH = 7.80) at 55 °C (A) at *t* = 0 min (blue) and *t* = 90 min (black). B: Photometric monitoring of the irradiation of **1** (*c* = 20 µM, PBS solution, pH = 7.80, orange) to the cylcoadducts **c1**^{shh}, **c1**^{sht}, and **[4]**$_2^{shh}$ (λ_{ex} =365 nm, *t* = 60 s, blue) and further irradiation at 270 nm *t* = 18 min (black). Inset A: Magnification of the absorption bands of the photocycloadducts of **1** upon thermal treatment.

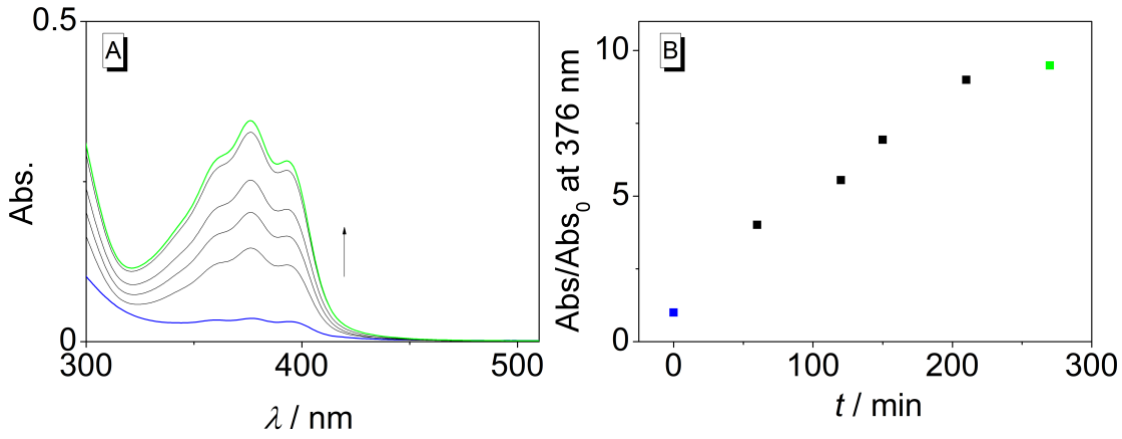

Figure S9. Photometric monitoring (A) of treatment of photocylcoadducts **c1**^{shh}, **c1**^{sht}, and **[4]**$_2^{shh}$ in PBS solution (20 µM, pH = 7.80, blue) with DTT (10 mM) to **4** (green) at 37 °C and change of absorbance at 376 nm over time (B).

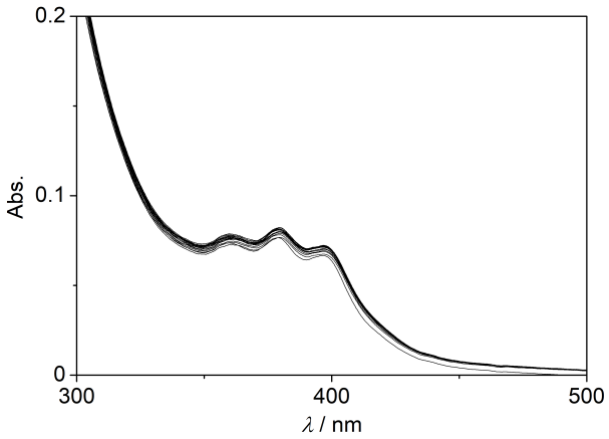

Figure S10. Photometric monitoring of thermal treatment (*t* = 16 h) of photocylcoadducts **c1**$^{\mathbf{shh}}$, **c1**$^{\mathbf{sht}}$, and **[4]**$_2^{\mathbf{shh}}$ (*c* = 20 µM, BPE solution, pH = 7.00) at 55 °C in the presence of ct DNA (40 µM).

^{1}H-NMR-spectroscopic investigations

A solution of the photoproducts of **1** (250 mL) with dithiothreitol (386 mg, 2.50 mmol, 10 mM) was stirred for 4 h at 45 °C under a nitrogen-gas atmosphere, and after cooling to room temperature an aq. solution of HPF_6 (60%, 2 mL) was added dropwise. The resulting solution was extracted immediately with CH_2Cl_2 (2 × 200 mL). The combined organic layers were washed with brine (1 × 50 mL) and dried with anhydrous Na_2SO_4. After filtration, the solvent was distilled under reduced pressure to give a yellow oil which was analyzed by ^{1}H-NMR spectroscopy. The formation of the thiol **4** as the major product was indicated by the characteristic shift and coupling pattern of the ^{1}H NMR signals of the sulfanylmethyl substituent, specifically the coupling between the methylene group (^3J = 4.02 ppm, 8 Hz) and thiol functionality (t, ^3J = 8 Hz).

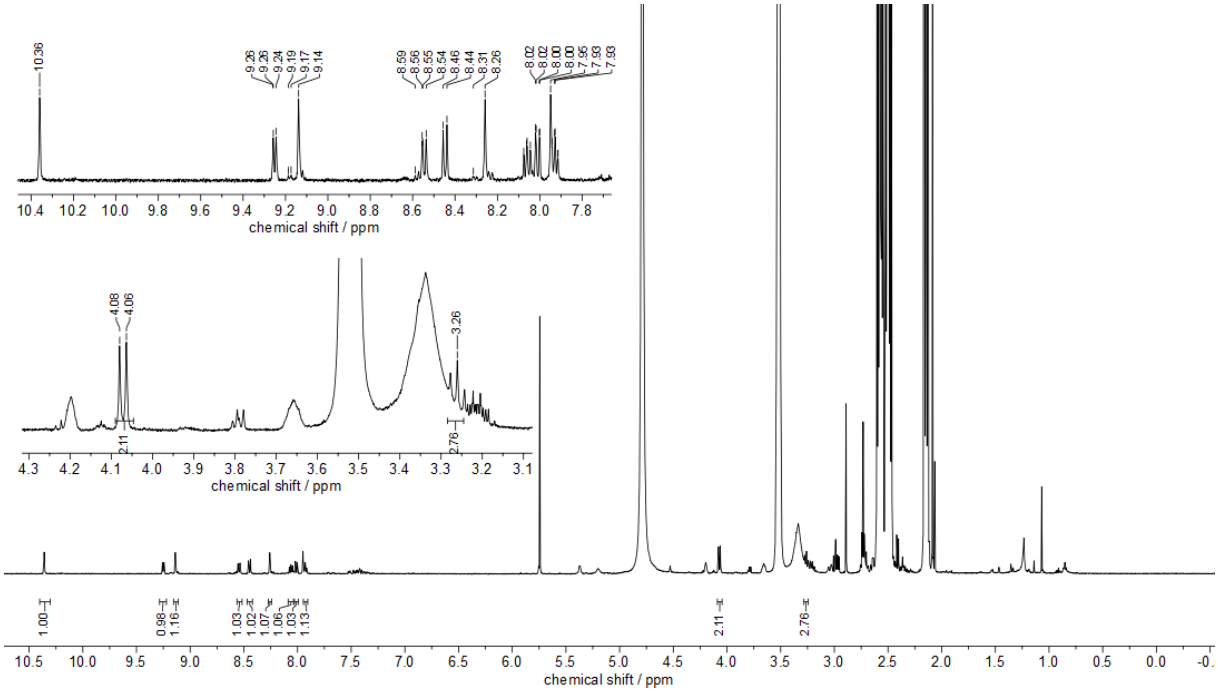

Figure S11. ^{1}H-NMR spectrum (600 MHz, DMSO-d_6, 25 °C) of the photoproducts of **1** (c = 40 µM, λ_{exc} = 365 nm for 19 min) after subsequent treatment with DTT (10 mM, 4 h, 45 °C).

5. DNA-binding properties

Photometric and fluorimetric titrations

To a solution of thioacetate **3** (c = 20 µM) in BPE buffer (pH = 7.00) were added aliquots of a ct DNA stock solution, and the respective absorption (Figure 4 A1) and emission (Figure S12, λ_{ex} = 403 nm) spectra were recorded after an equilibration time of three min.

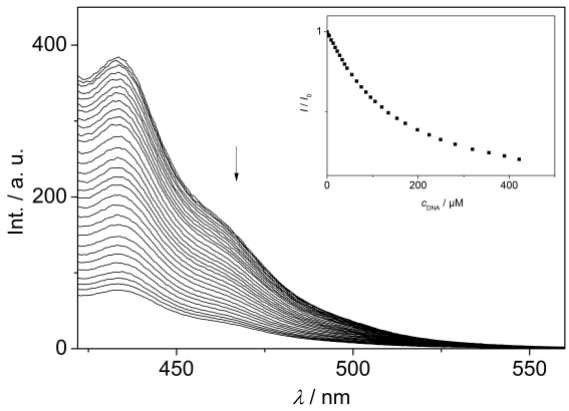

Figure S12. Fluorimetric titration (λ_{ex} = 403 nm) of **3** (c = 20 µM) in BPE buffer (pH = 7.00) with ct DNA. Inset: Plot of the relative fluorescence intensity I / I_0 versus c_{DNA}.

For ligand **1** a fluorescent indicator displacement (FID) experiment with thiazol orange (TO) was performed according to known procedure.[1] Thus, to a solution of TO (0.5 µM) with ct DNA (0.25 µM) in BPE buffer (pH = 7.00) were added aliquots of a stock solution of **1** (*c* = 50 µM, BPE buffer) and the fluorescence upon irradiation with λ_{ex} = 475 nm was recorded after an equilibration time of 3 min. The percentage displacement (PD) of TO and the PD50 value (PD = 50%) were calculated according to equation 1.

$$PD = 100 - \left(\frac{FA}{FA_0} \times 100\right) \qquad \text{(eq. 1)}$$

The variable FA refers to the fluorescence area (500–750 nm) at the respective titration step and FA_0 refers to the fluorescence area before the addition of the ligand **1**.

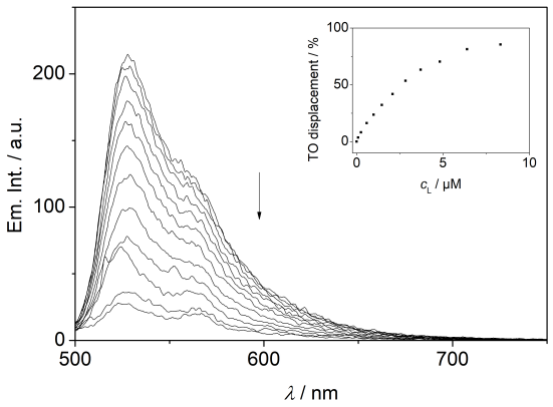

Figure S13. Changes of the fluorescence spectra (λ_{ex} = 475 nm) of thiazole orange (0.5 µM) bound to DNA (0.25 µM) upon addition of **1** in BPE buffer (pH = 7.00). Inset: TO displacement versus concentration of the added ligand.

CD- and LD-spectroscopic analysis

Solutions of ct DNA (*c* = 50 µM) with different concentrations of thioacetate **3** (BPE buffer pH = 7.0), disulfide **1** (BPE buffer pH = 7.0), and thiol **4** [BPE buffer pH = 7.80, in the presence of dithiothreitol (DTT), *c* = 10 mM] in the respective buffer solution were analyzed by CD and LD spectroscopy. Prior to the addition of DNA, the solutions of **4** were treated for 5 h at 37 °C with the reducing agents under a nitrogen atmosphere and under exclusion of light. Analogously, the solutions of the photoproducts of **1** were prepared from irradiation of **1** (λ_{ex} = 365 nm, *t* = 3 min) prior to the addition of DNA.

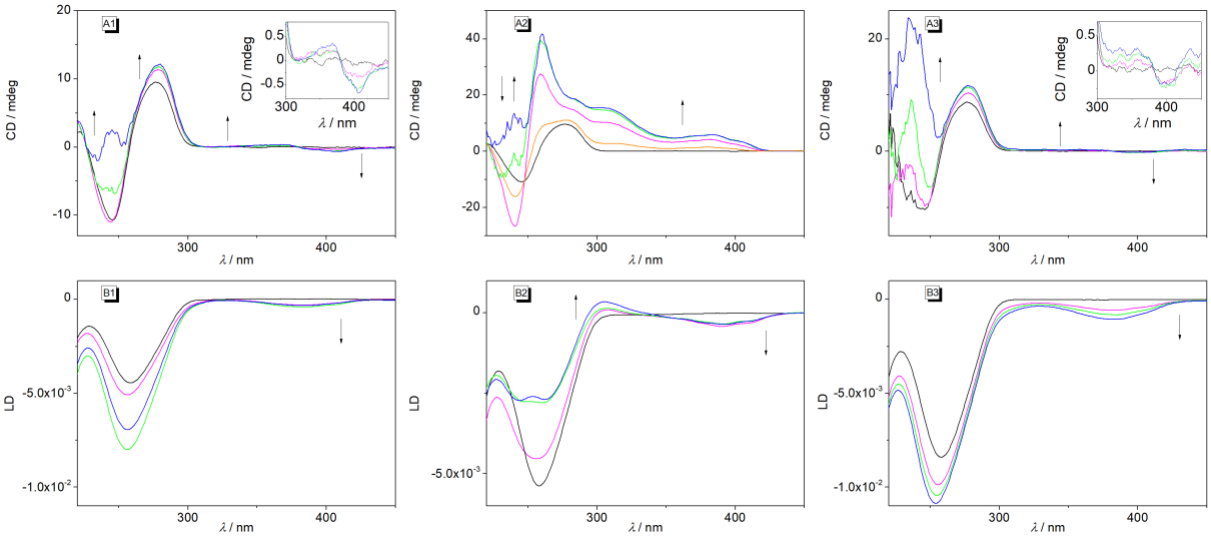

Figure S14. Polarimeric DNA titrations (CD: A1–3, LD: B1–3) of **3** (1), **1** (2) and **4** [3, in the presence of dithiothreitol (DTT), *c* = 10 mM] with ct DNA (*c* = 50 µM); in BPE buffer (1, 2, pH = 7.0; 3, pH = 7.8 with DTT *c* = 10 mM); *LDR* = 0 (black), 0.1 (orange), 0.5 (magenta), 1.0 (green), 1.5 (blue). Inset: Magnification of the ICD bands in the absorption range of the ligands. The arrows indicate the change of the CD/LD signal with increasing *LDR*.

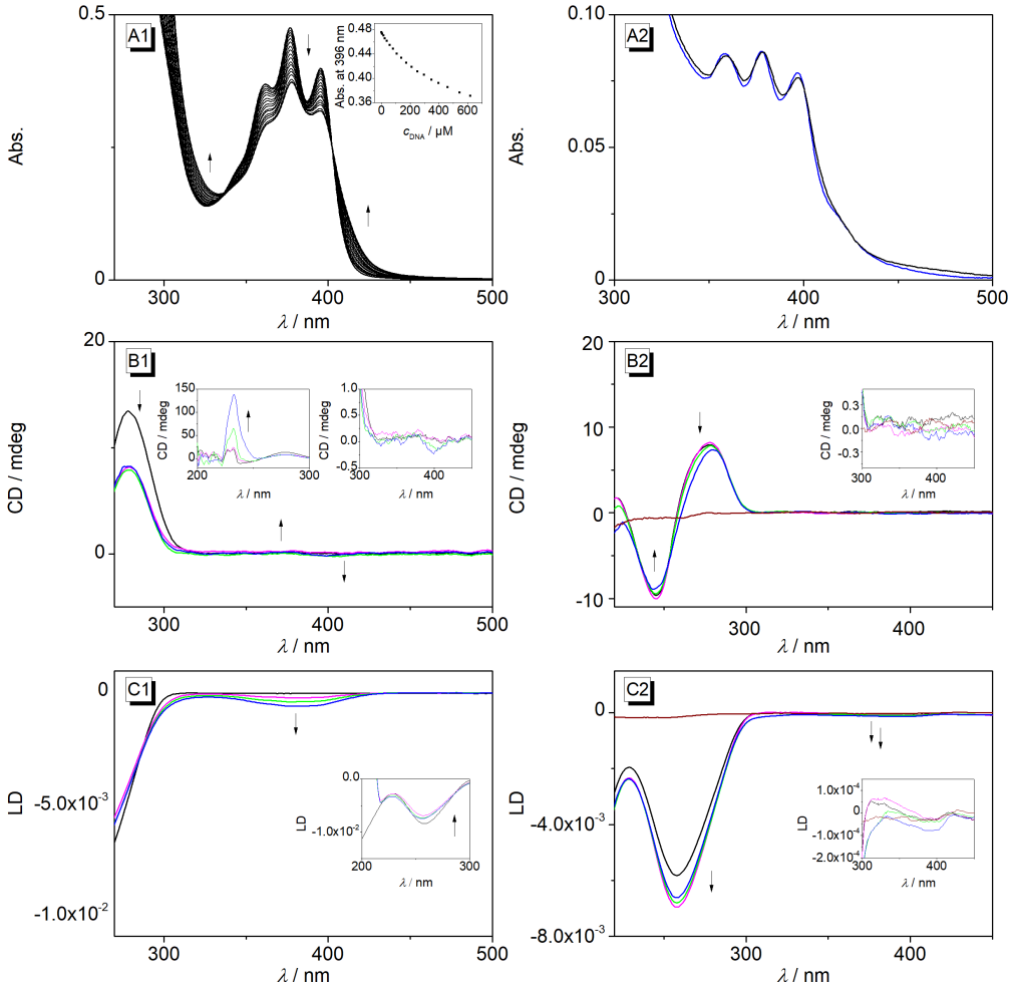

Figure S15. Photometric (A) and polarimetric (CD: B, LD: C) DNA titrations of **4** [(1, *c* = 40 µM) in the presence of l-glutathione (GSH), *c* = 10 mM] and of the photoproducts of **1** (2, *c* = 53 µM, blue) with ct DNA (351 µM, black, B1); in phosphate buffer (**1**, pH = 7.0; **4**, pH = 7.8). CD/LD: *LDR* = 0 (black), 0.1 (orange), 0.5 (magenta), 1.0 (green), 1.5 (blue). The arrows indicate the change of the absorbance upon addition of DNA (A) or the change of the CD/LD signal with increasing *LDR* (B, C).

Analogously to the photometric titrations, a polarimetric DNA titration was performed with the disulfide **1**. Hence, to a solution of DNA (*c* = 50 µM) in BPE buffer (pH =7.00) were added aliquots of a solution of **1** in BPE buffer. The resulting binding isotherms were fitted to the theroretical model (eq. 2 and 3).[2,3]

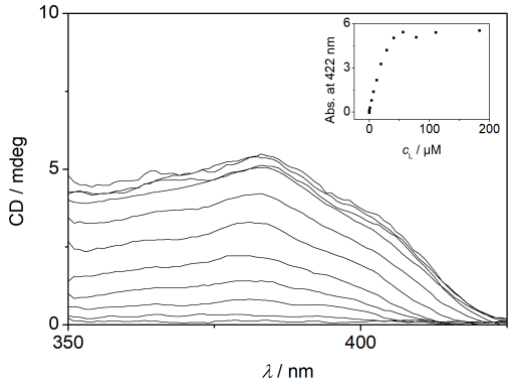

Figure S16. Polarimetric DNA titration of **1** (c_{DNA} = 50 µM) in BPE buffer (pH = 7.00). Insets: Plots of the intensity of the CD signal at 422 nm versus ligand concentration.

Determination of binding constants

The binding constants were determined by fitting of the respective saturation fraction (SF, eq. 2) calculated from the photometric titrations according to literature protocol (eq. 3.).[3]

$$SF = \frac{Abs_n - Abs_0}{Abs_s - Abs_0} \qquad \text{(eq. 2)}$$

The variable Abs_n is the absorption at the titration step n, Abs_0 is the absorption with n = 0 and Abs_s is the absorption when all ligands are bound to the DNA (assessed by analysis of photometric data, often last titration step).

$$y = \frac{1}{2} R\,(A + B + x - \sqrt{(((A + B + x)^2) - (4Bx))}\,) \qquad \text{(eq. 3)}$$

The variable R refers to an instrumental response sensitivity dependent variable, A is the reciprocal binding constant K_b, B is a dependent variable and is equal to the concentration of the ligand or the DNA (equal to ligand concentration if DNA is added to the ligand and vice versa), however, the value can be adjusted according to available binding sites, e.g. if the ligand (c = 20 µM) binds only to every third binding site within the DNA the value of B must be set to 6.00×10^{-5}.

Table S1. Parameters of the fit of experimental titration data to the theoretical model (eq. 2, Figure S16).

Ligand (reductant)	A[d]	B[e]	R[f]
1[a]	3.12×10^{-6}	2.50×10^{-5}	4.07×10^{4}
4 (GSH)[b]	4.04×10^{-4}	4.00×10^{-5}	4.18×10^{4}
4 (DTT)[b]	2.50×10^{-4}	4.00×10^{-5}	3.52×10^{4}
3[c]	1.15×10^{-4}	6.00×10^{-5}	2.17×10^{4}

[a] Derived from polarimetric DNA titration (CD spectroscopy). [b] Derived from photometric DNA titration. For ligand **4**, the reagent that was used for the reduction of **1** is given. [c] Derived from photometric titration. [d] Dependent variable A = K_b^{-1}. [e] Independent variable, fixed according to concentration of the ligand/DNA and theoretically available binding sites. [f] Dependent instrumental response sensitivity variable.

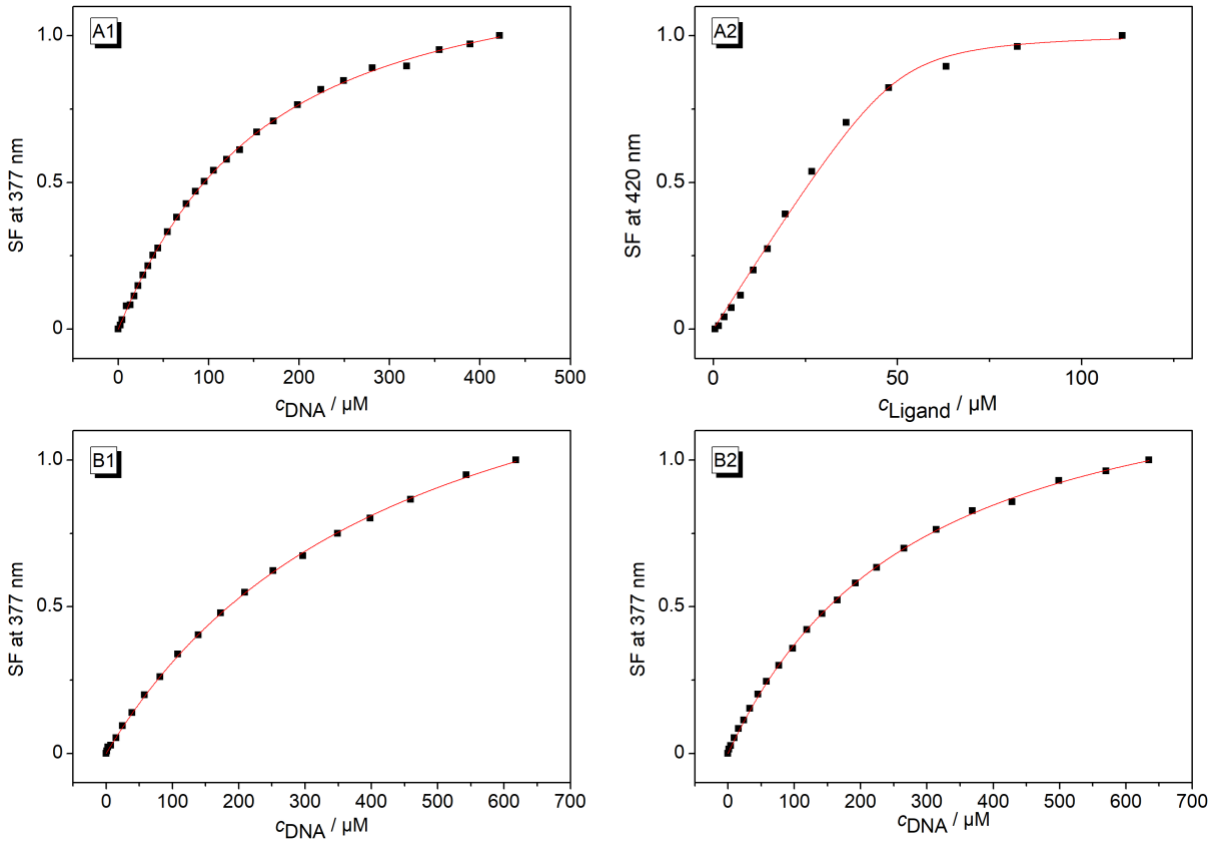

Figure S17. Binding isotherms of complexes of **3** (A1), **1** (A2), **4** (obtained by reduction of **1** by GSH, B1, obtained by reduction of **1** by DTT, B2) with DNA represented as plots of SF versus DNA concentration. The lines represent the best fit of the experimental data to the theoretical model (Levenberg–Marquardt least-square fitting curves).[3]

6. Illustration of the proposed binding mode of 1 with DNA

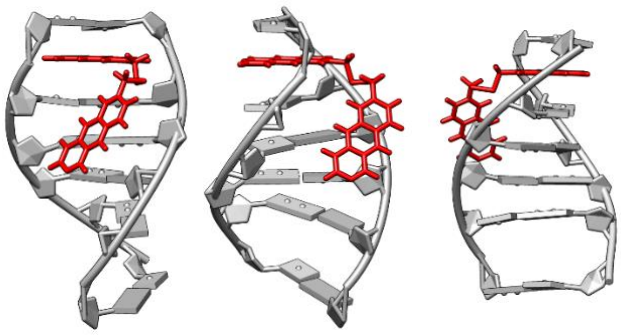

Figure S18. Raw sketch (no calculation) of the proposed binding mode of **1** with DNA. The structure of the duplex DNA was taken from a known ellipticine-DNA complex (from Protein Data Base; DOI: https://www.rcsb.org/structure/1z3f). The ellipticine ligands were removed from the intercalation sites and, in one case, substituted with **1** without further energy minimization.

7. NMR spectra

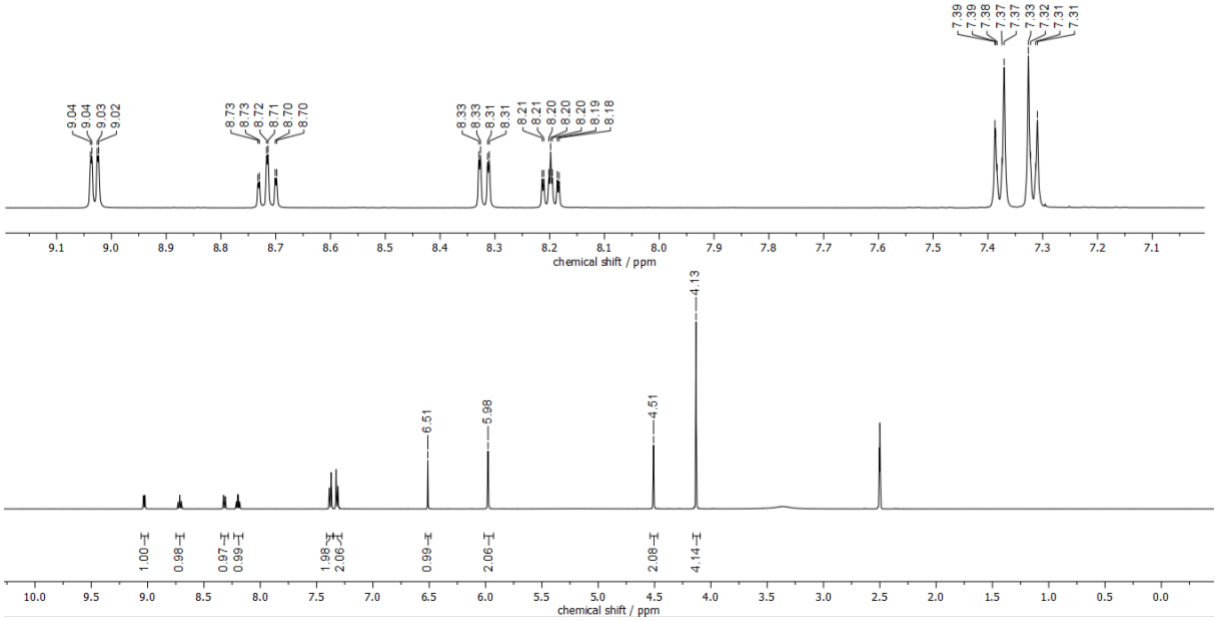

Figure S19. ^{1}H-NMR spectrum (500 MHz, DMSO-d_6, 25 °C) of **7**.

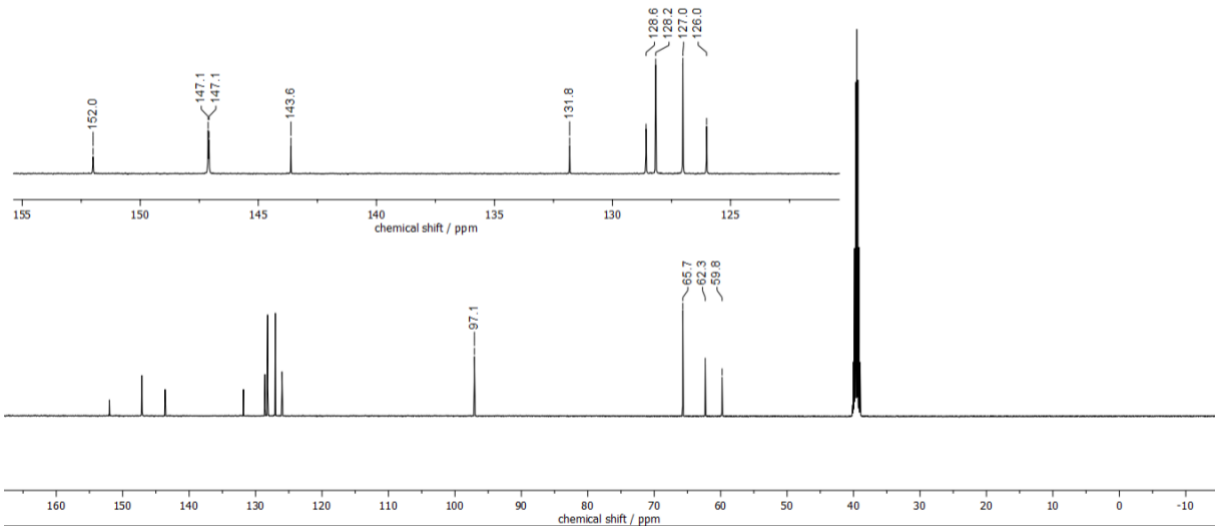

Figure S20. ^{13}C-NMR spectrum (125 MHz, DMSO-d_6, 25 °C) of **7**.

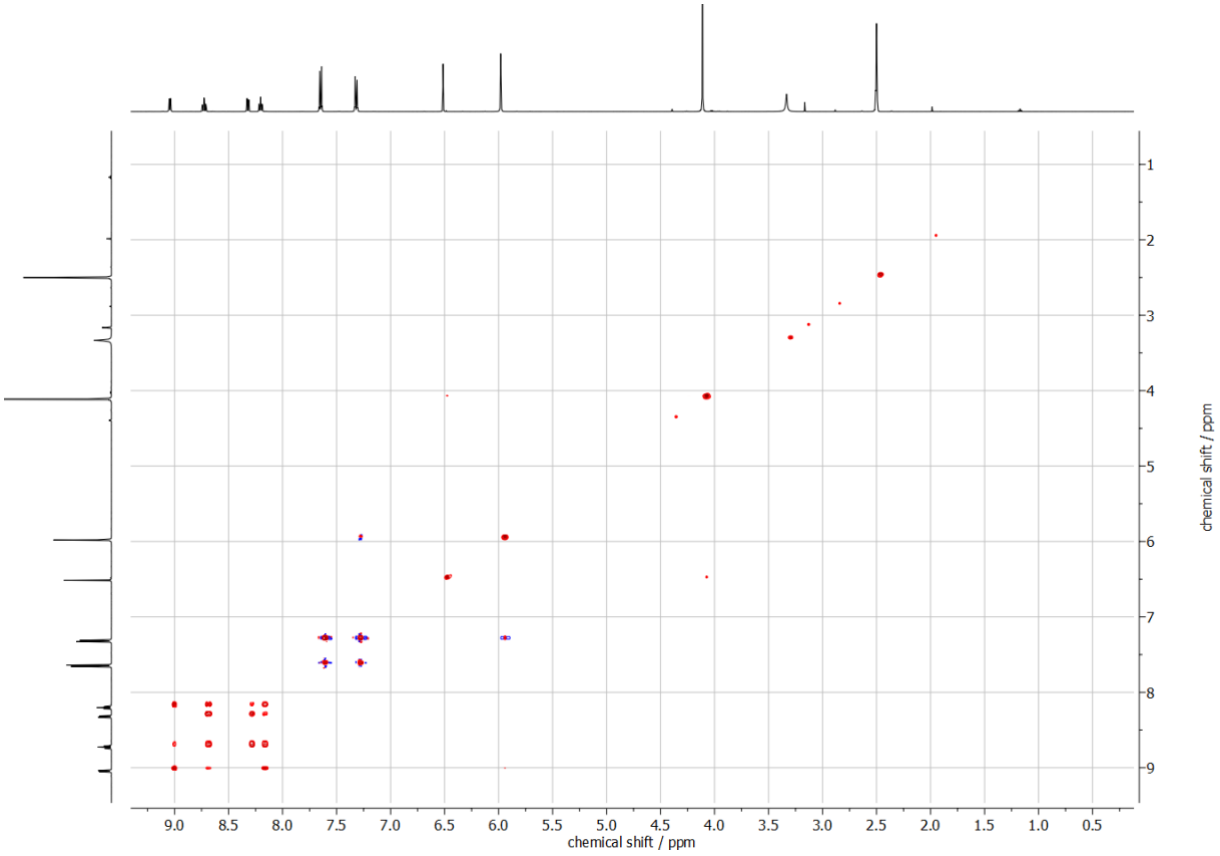

Figure S21. HH-COSY spectrum (500 MHz, DMSO-d_6, 25 °C) of **7**.

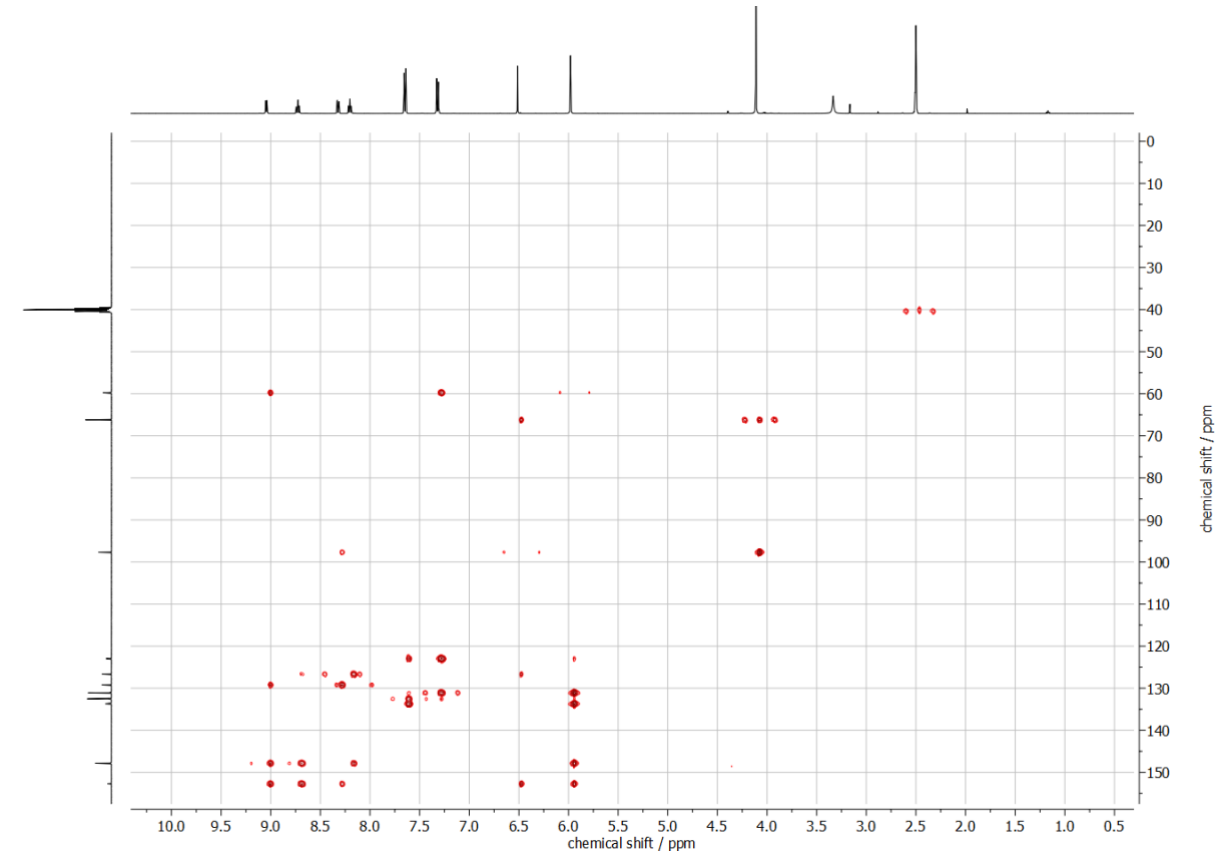

Figure S22. HSQC spectrum (500 MHz, DMSO-d_6, 25 °C) of **7**.

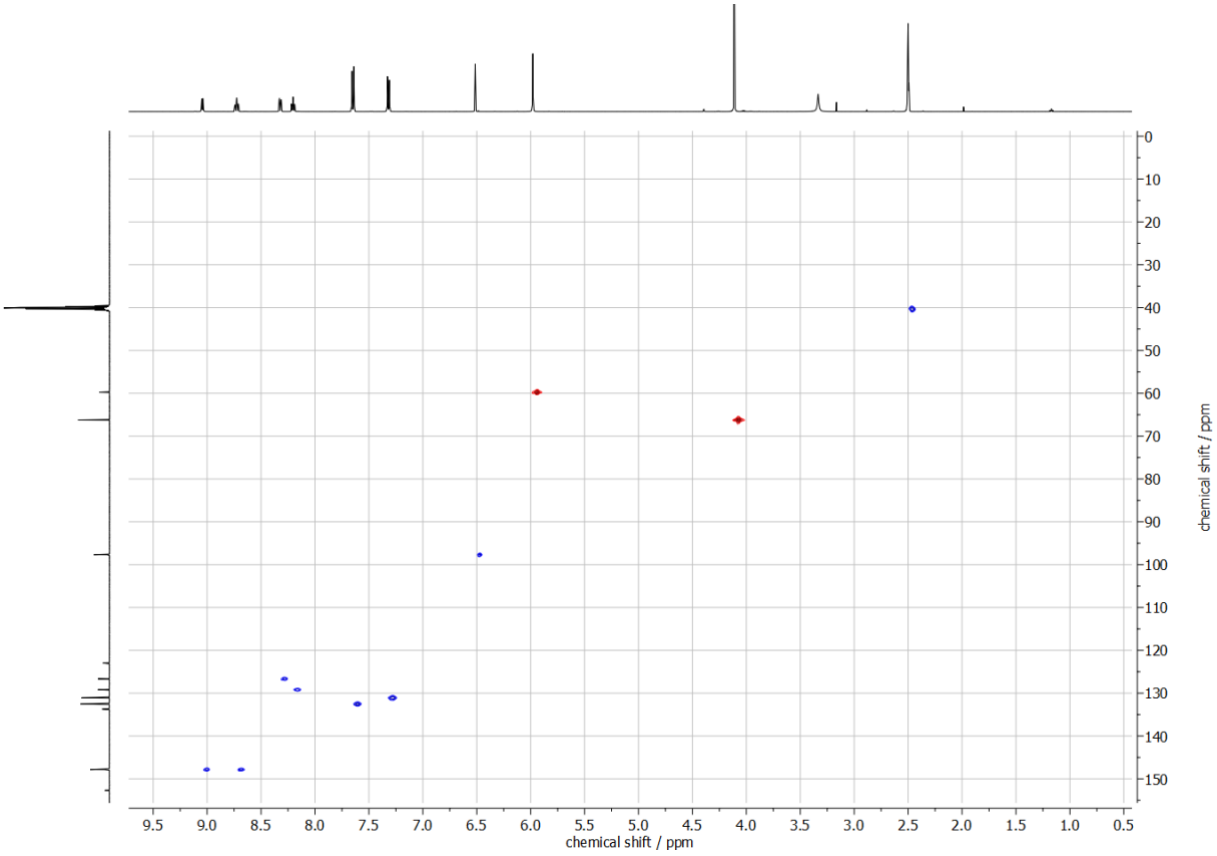

Figure S23. HMBC spectrum (500 MHz, DMSO-d_6, 25 °C) of **7**.

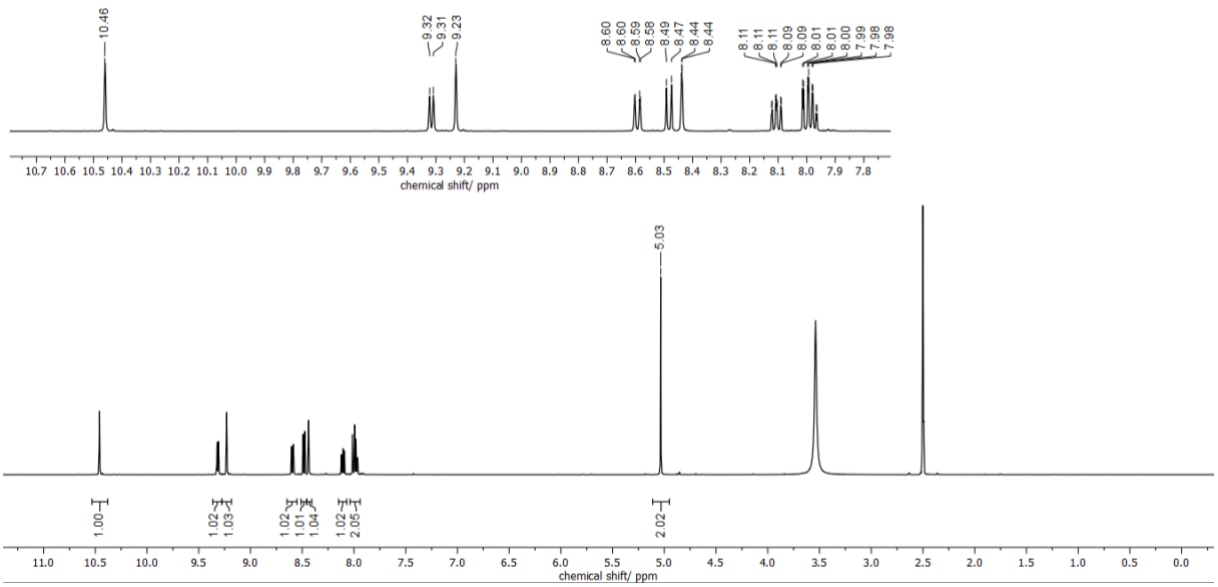

Figure S24. ^{1}H-NMR spectrum (500 MHz, DMSO-d_6, 25 °C) of **2**.

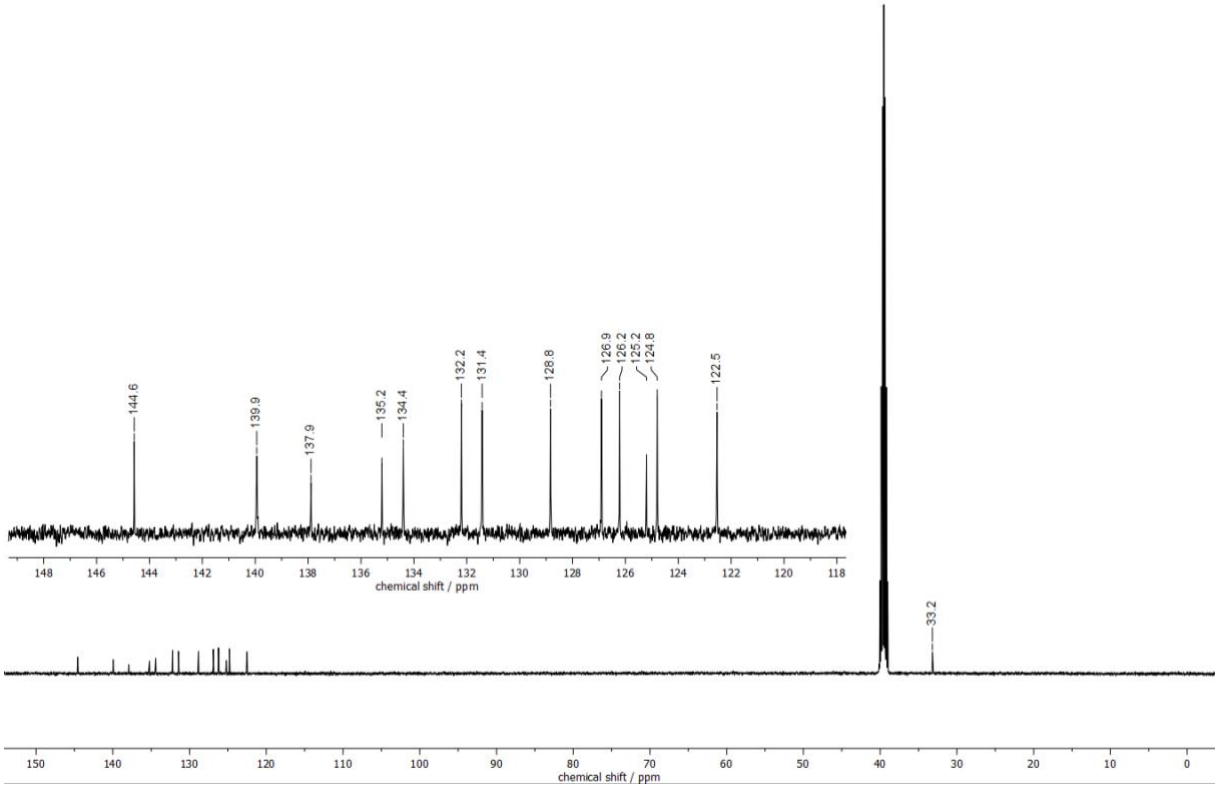

Figure S25. ^{13}C-NMR spectrum (125 MHz, DMSO-d_6, 25 °C) of **2**.

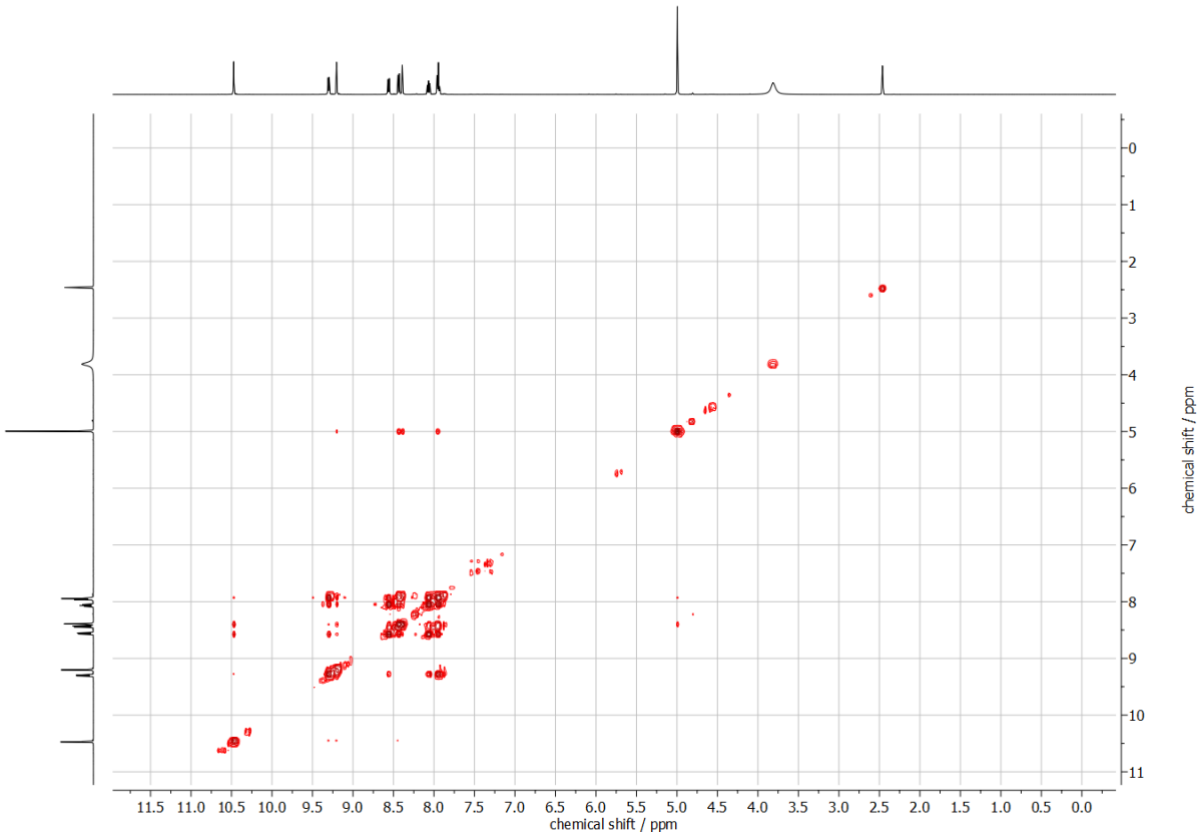

Figure S26. HH-COSY spectrum (500 MHz, DMSO-d_6, 25 °C) of **2**.

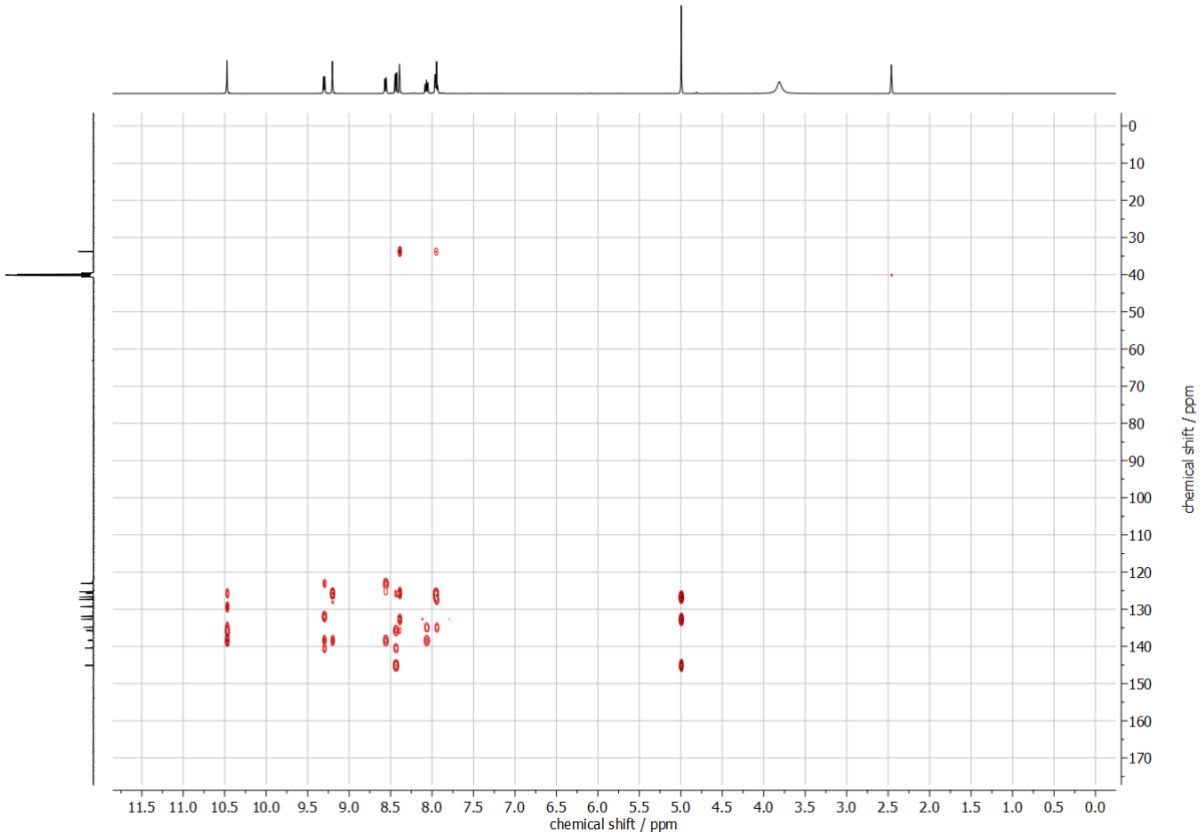

Figure S27. HSQC spectrum (500 MHz, DMSO-d_6, 25 °C) of **2**.

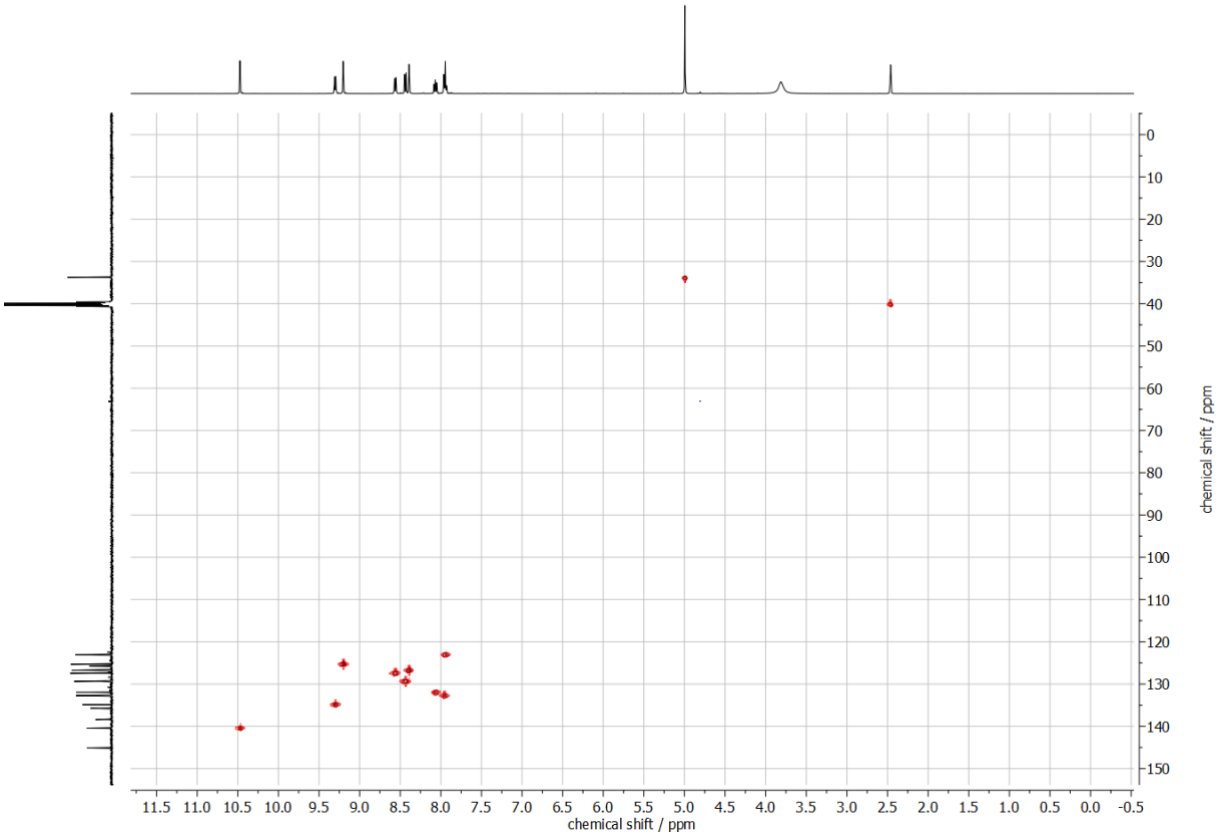

Figure S28. HMBC spectrum (500 MHz, DMSO-d_6, 25 °C) of **2**.

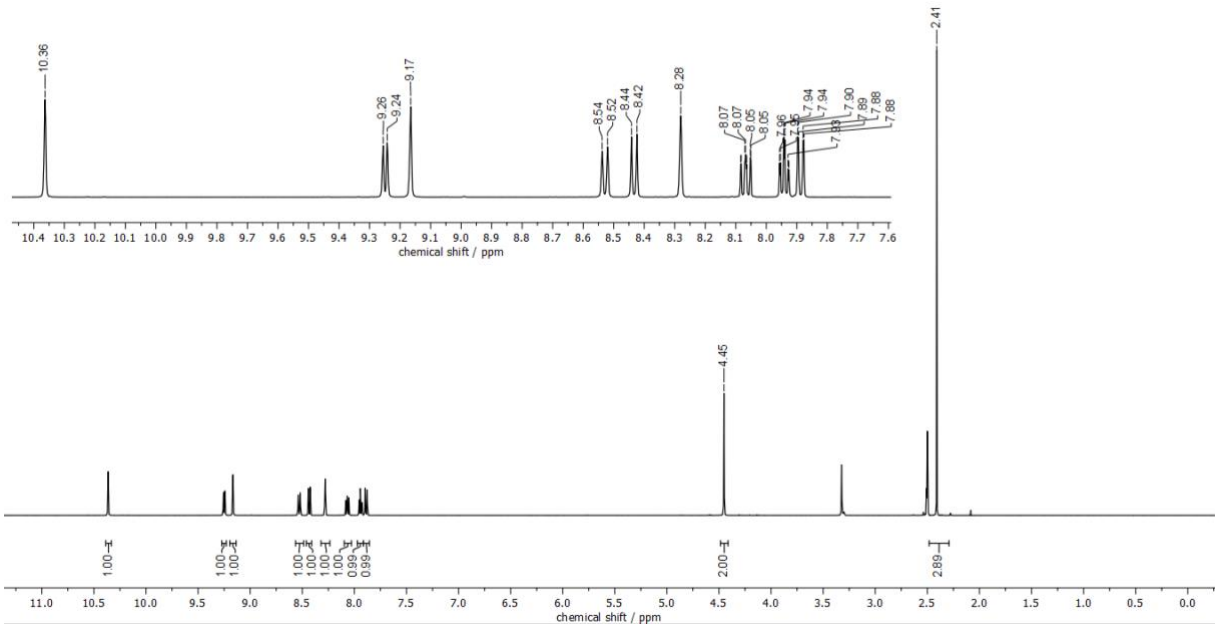

Figure S29. ^{1}H-NMR spectrum (500 MHz, DMSO-d_6, 25 °C) of **3**.

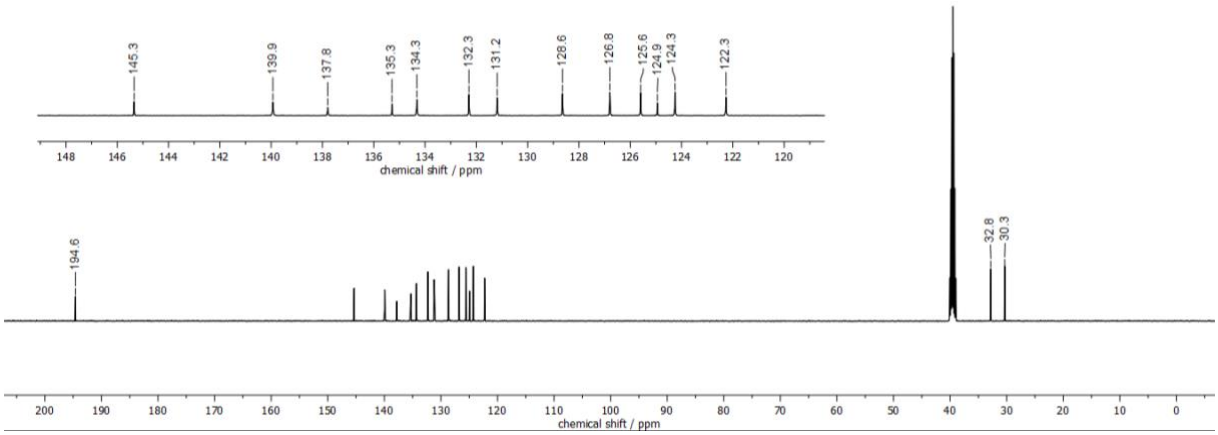

Figure S30. ^{13}C-NMR spectrum (125 MHz, DMSO-d_6, 25 °C) of **3**.

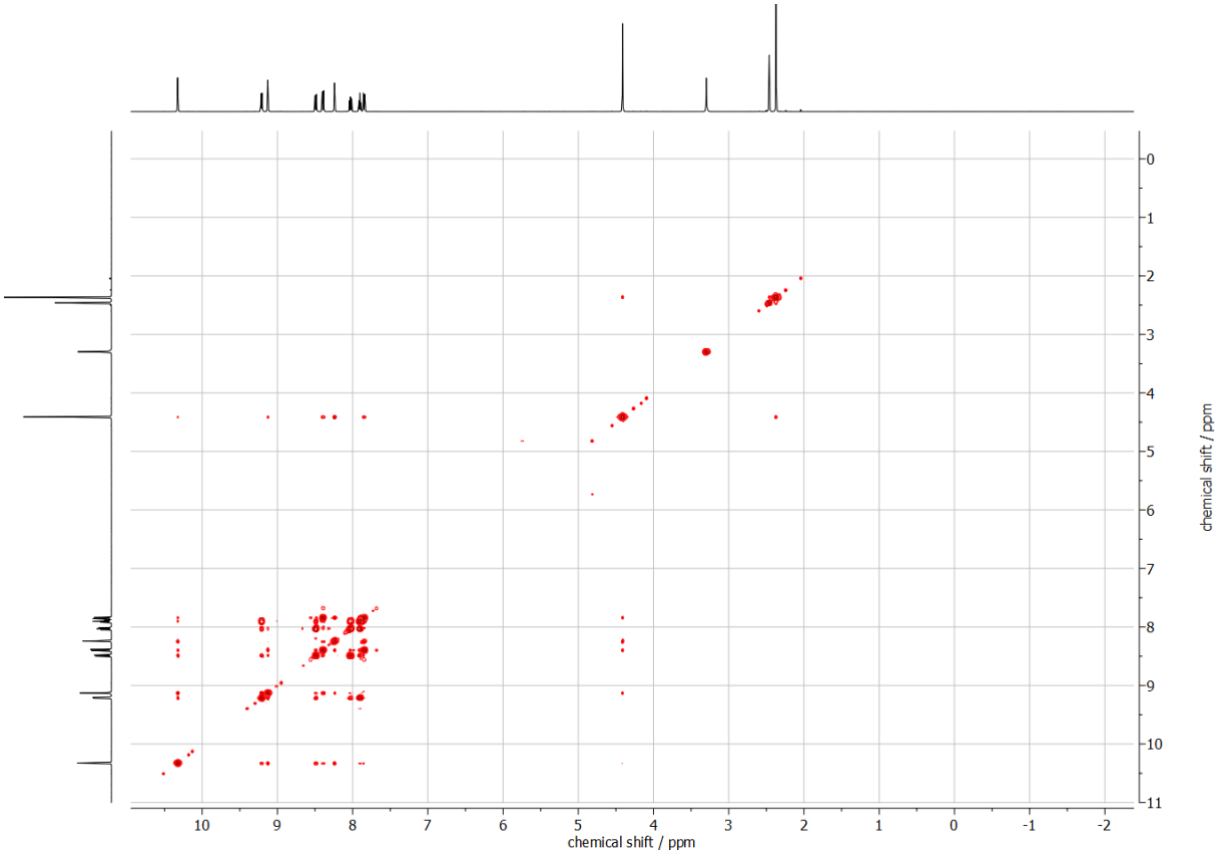

Figure S31. HH-COSY spectrum (500 MHz, DMSO-d_6, 25 °C) of **3**.

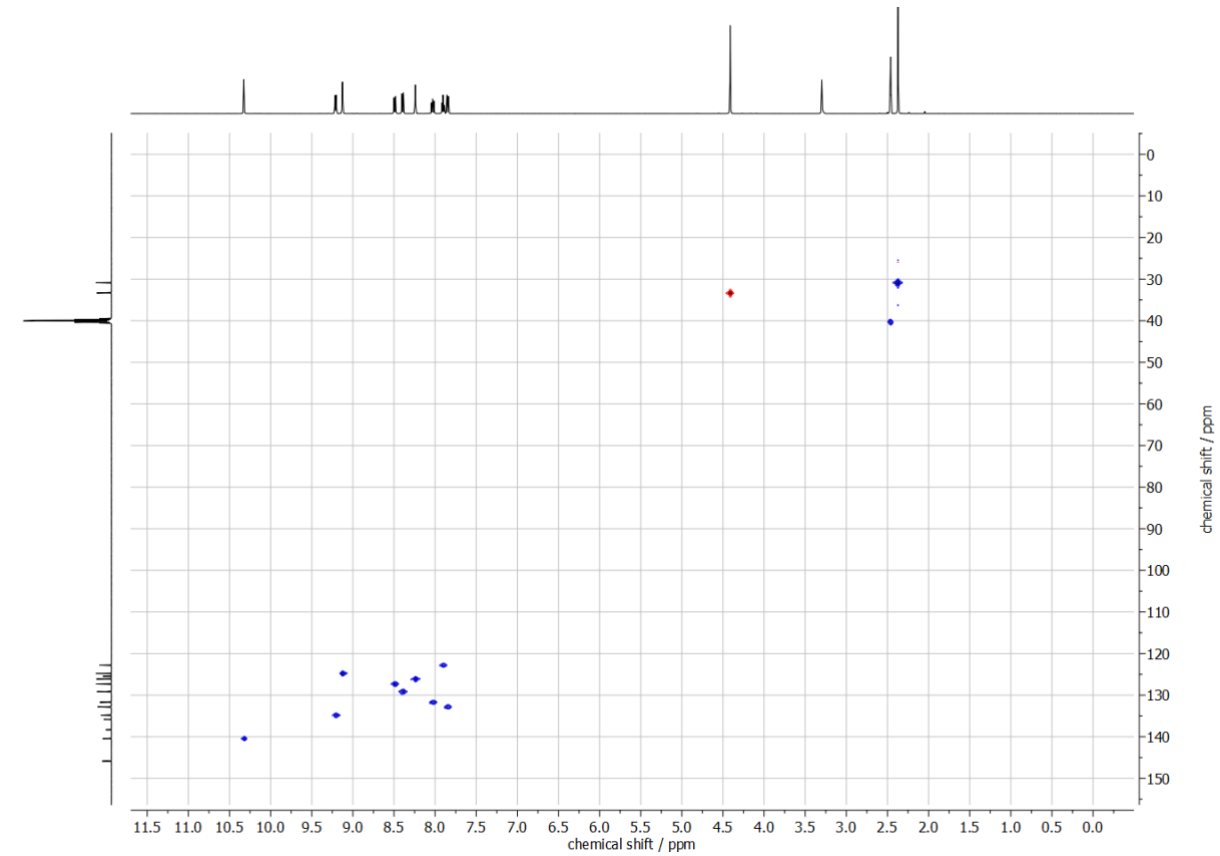

Figure S32. HSQC spectrum (500 MHz, DMSO-d_6, 25 °C) of **3**.

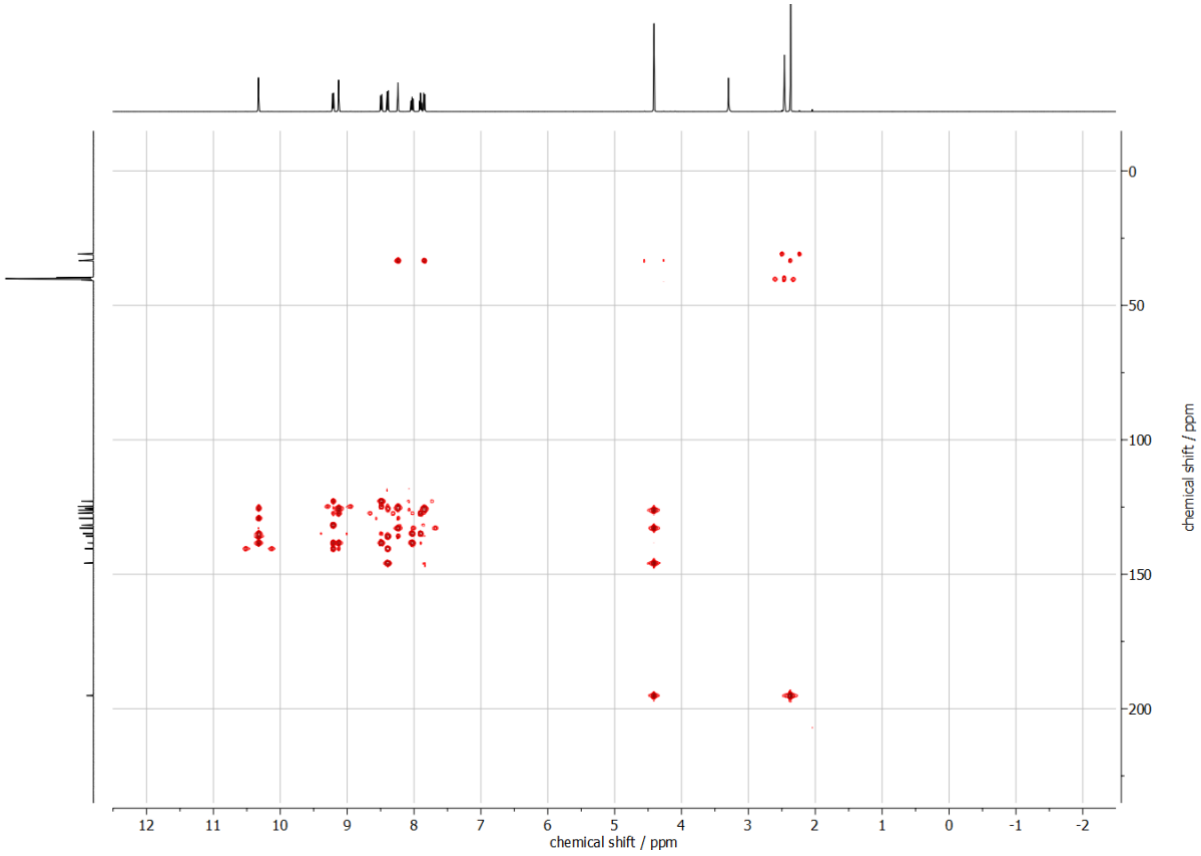

Figure S33. HMBC spectrum (500 MHz, DMSO-d_6, 25 °C) of **3**.

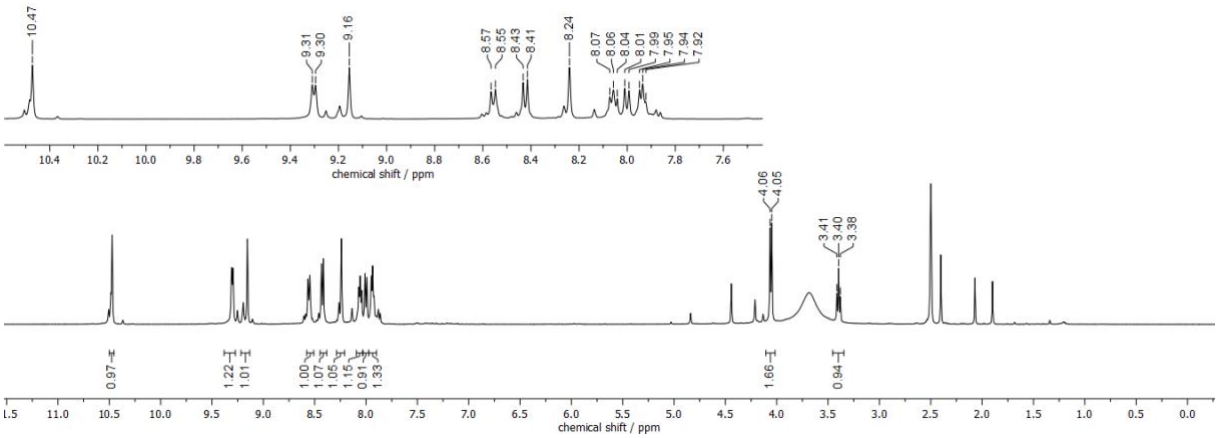

Figure S34. Crude ^{1}H-NMR spectrum (500 MHz, DMSO-d_6, 25 °C) of **4**.

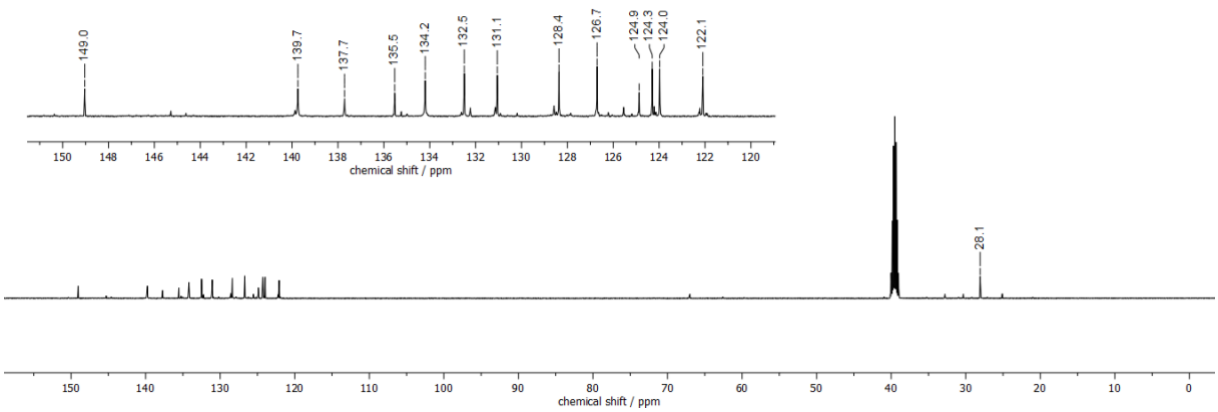

Figure S35. Crude ^{13}C-NMR spectrum (125 MHz, DMSO-d_6, 25 °C) of **4**.

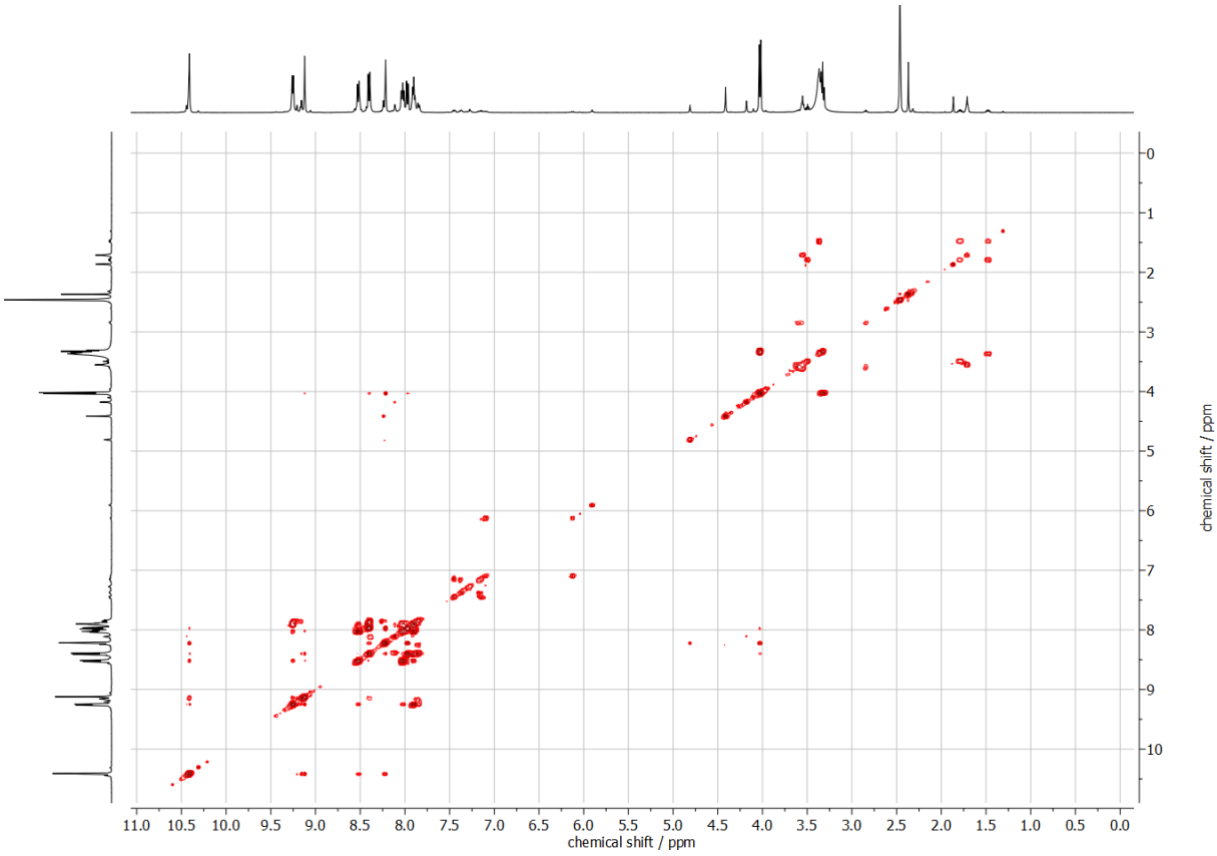

Figure S36. Crude HH-COSY spectrum (500 MHz, DMSO-d_6, 25 °C) of **4**.

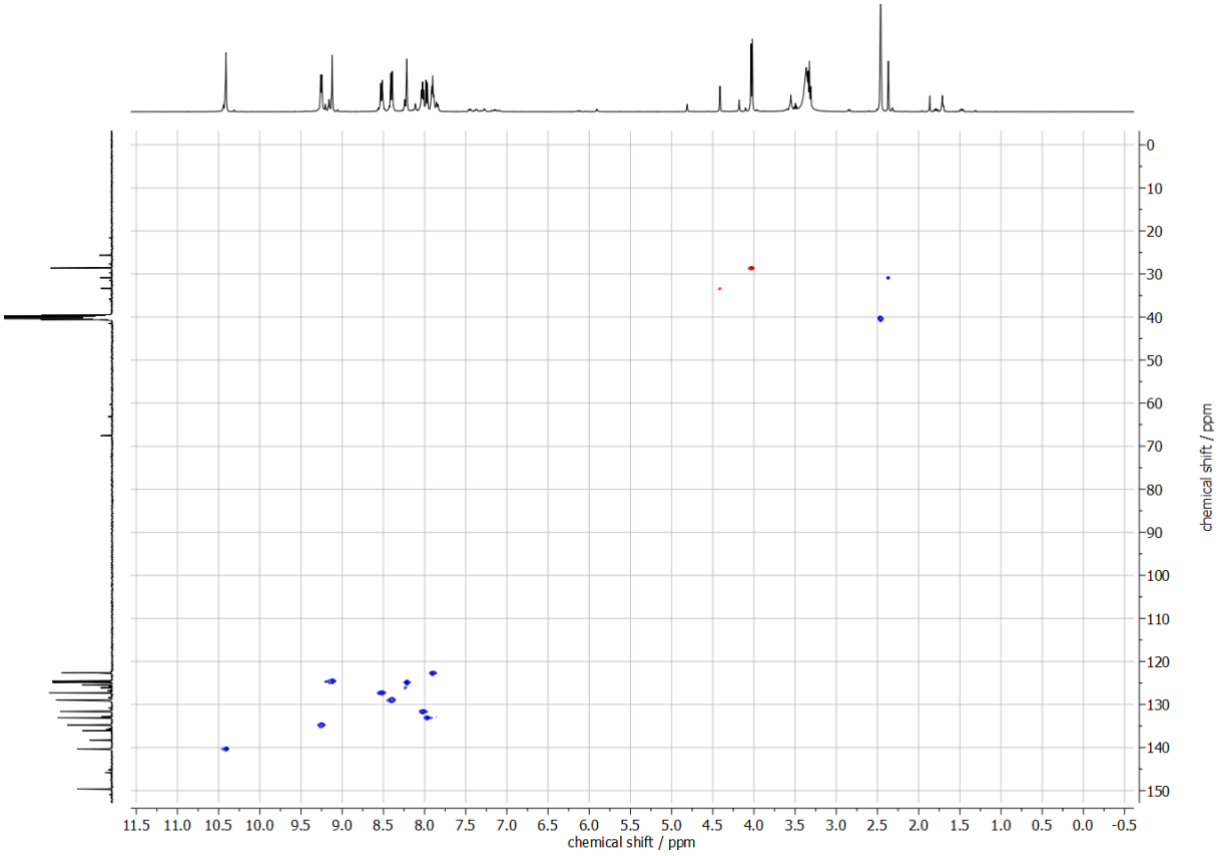

Figure S37. Crude HSQC spectrum (500 MHz, DMSO-d_6, 25 °C) of **4**.

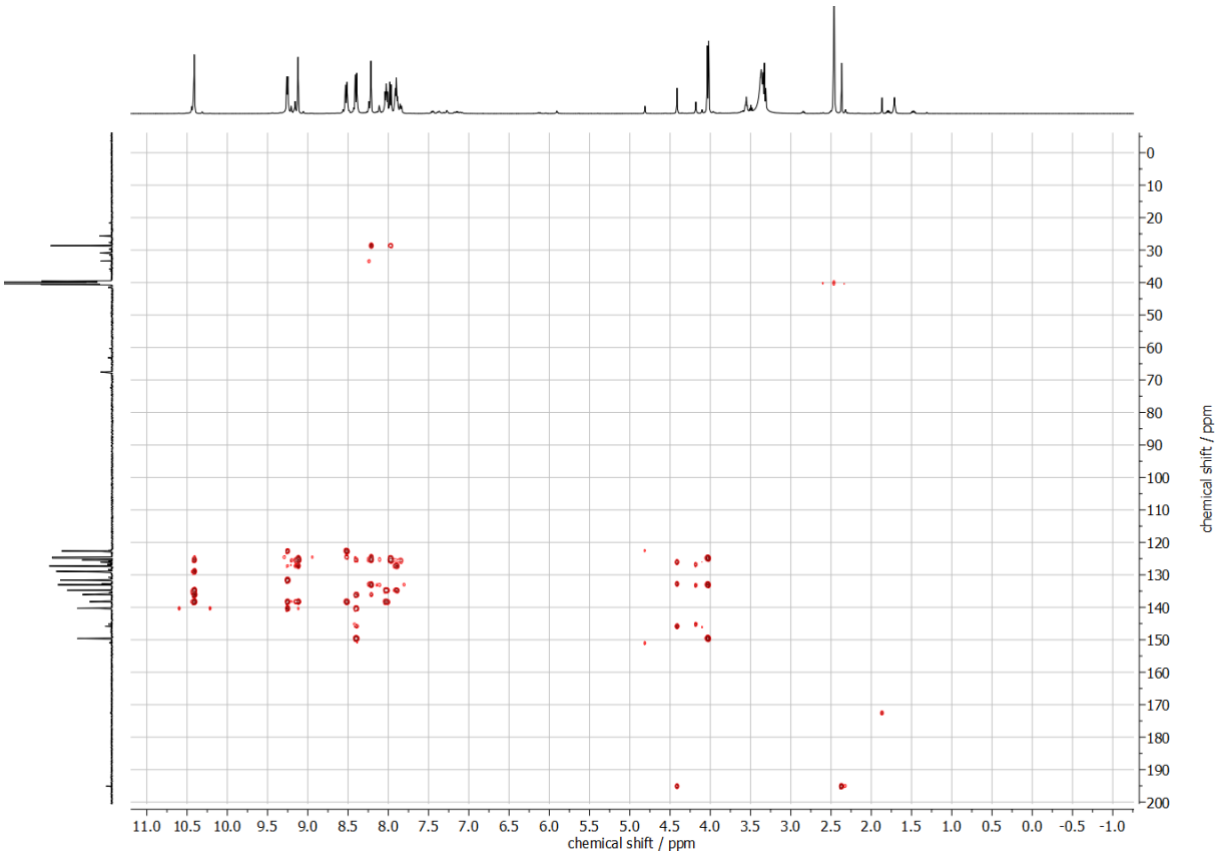

Figure S38. Crude HMBC spectrum (500 MHz, DMSO-d_6, 25 °C) of **4**.

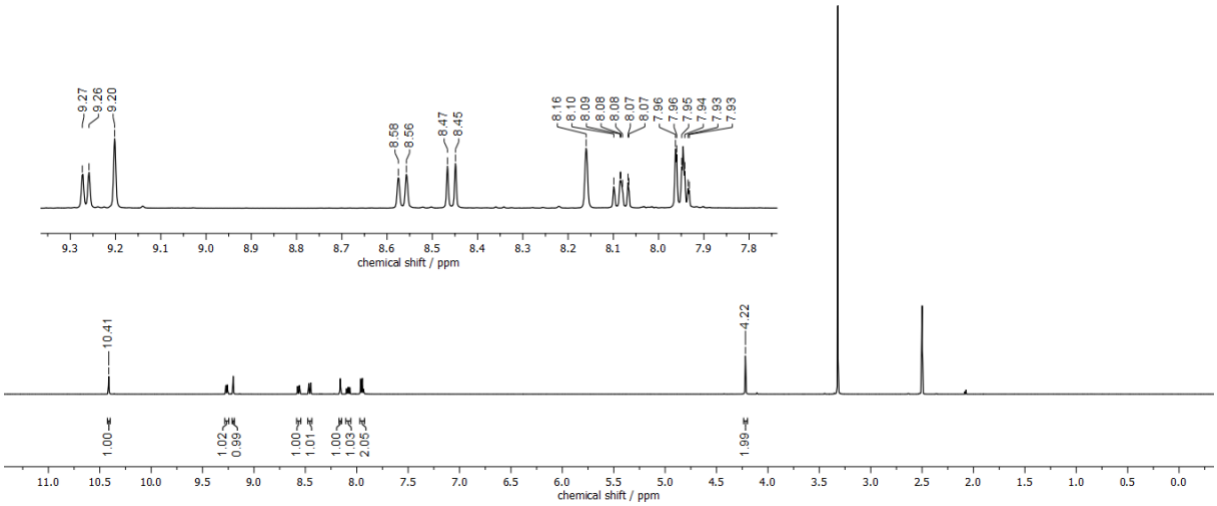

Figure S39. ^{1}H-NMR spectrum (500 MHz, DMSO-d_6, 25 °C) of **1**.

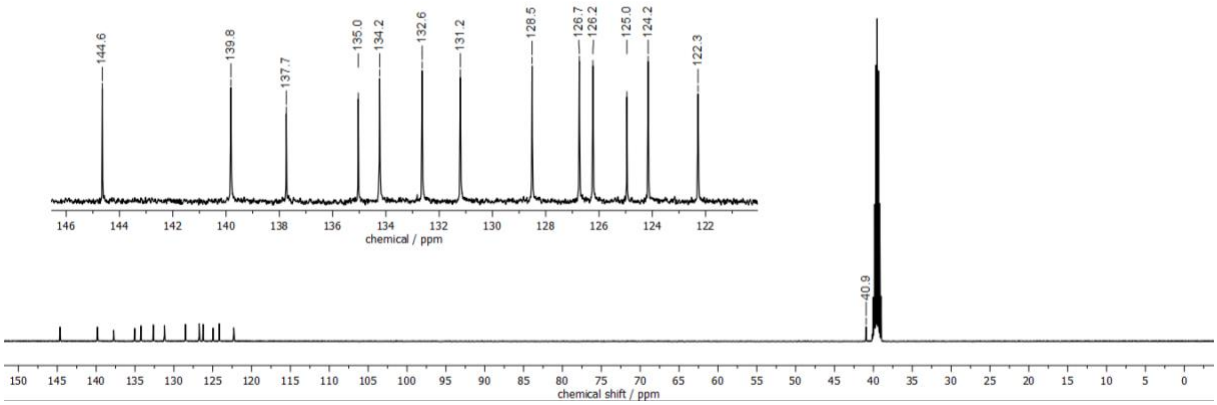

Figure S40. ^{13}C-NMR spectrum (125 MHz, DMSO-d_6, 25 °C) of **1**.

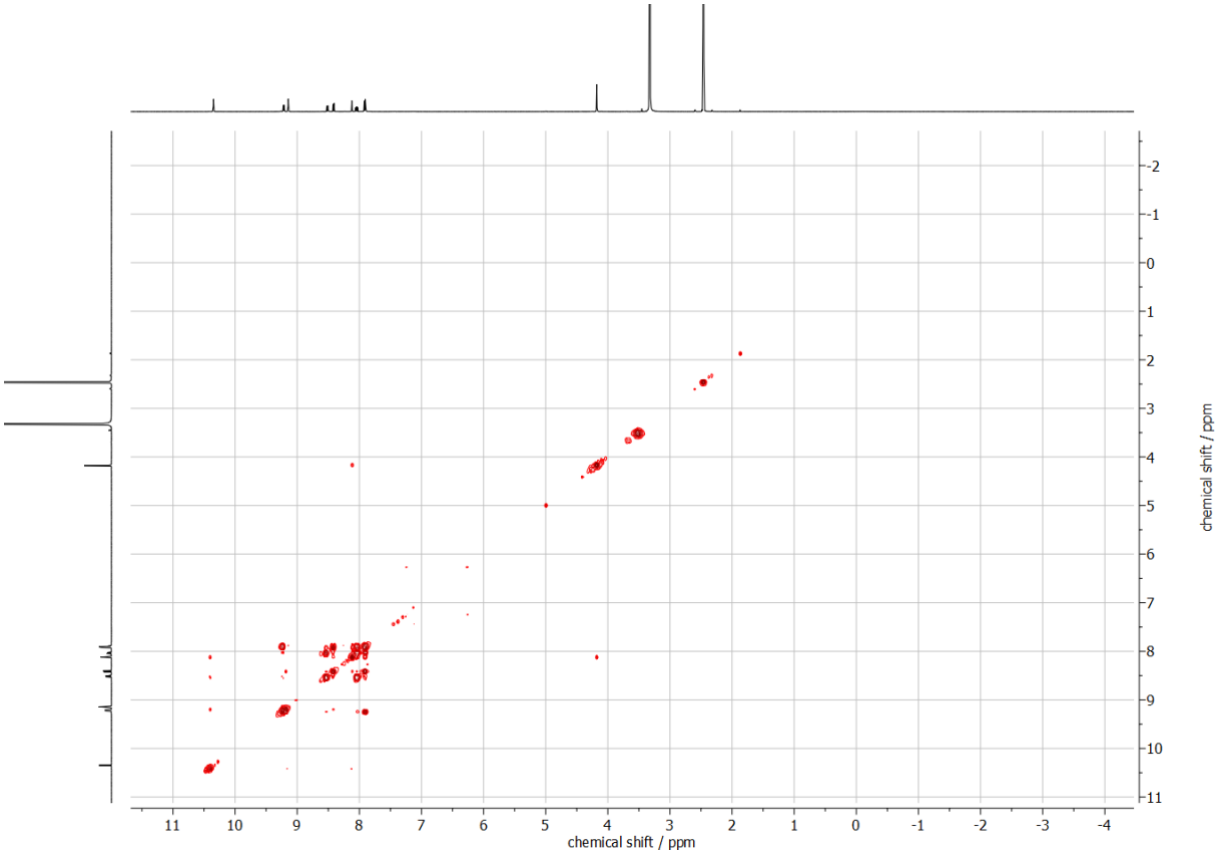

Figure S41. HH-COSY spectrum (500 MHz, DMSO-d_6, 25 °C) of **1**.

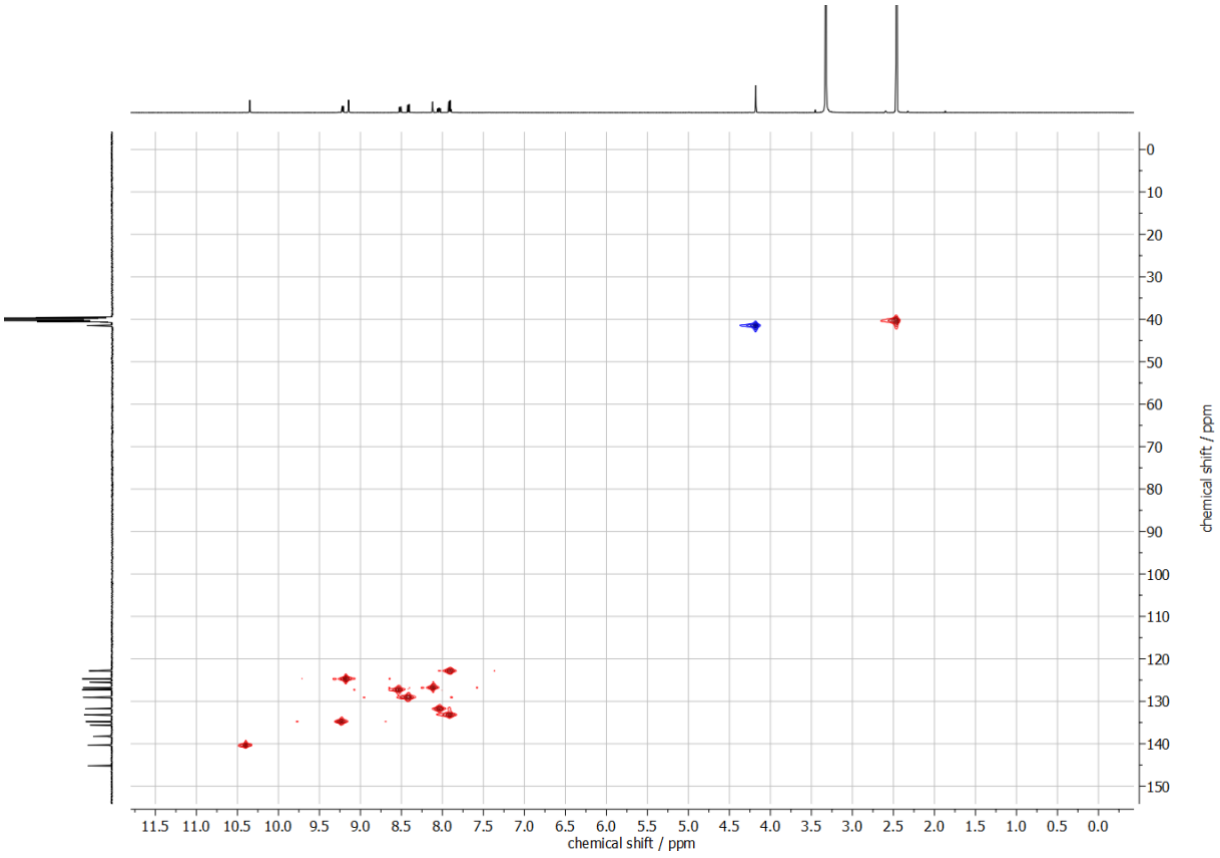

Figure S42. HSQC spectrum (500 MHz, DMSO-d_6, 25 °C) of **1**.

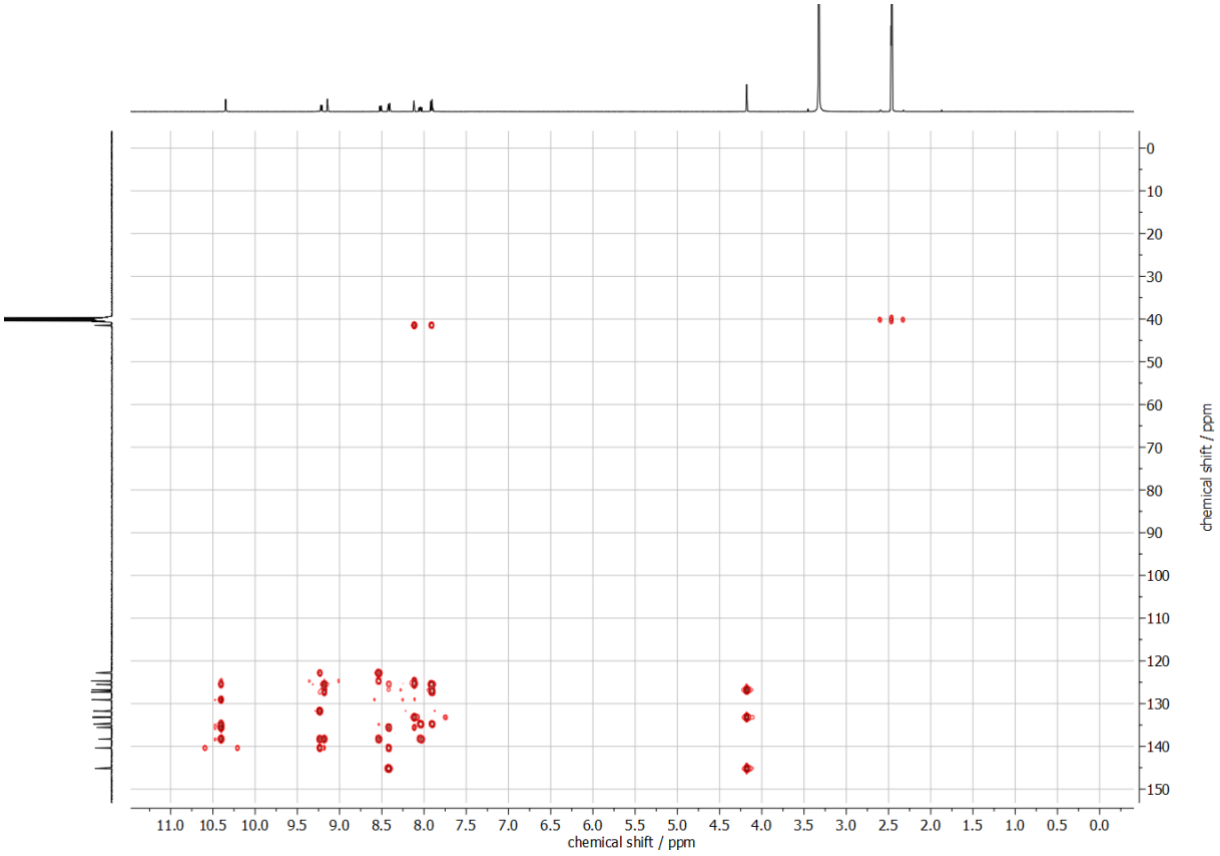

Figure S43. HMBC spectrum (500 MHz, DMSO-d_6, 25 °C) of **1**.

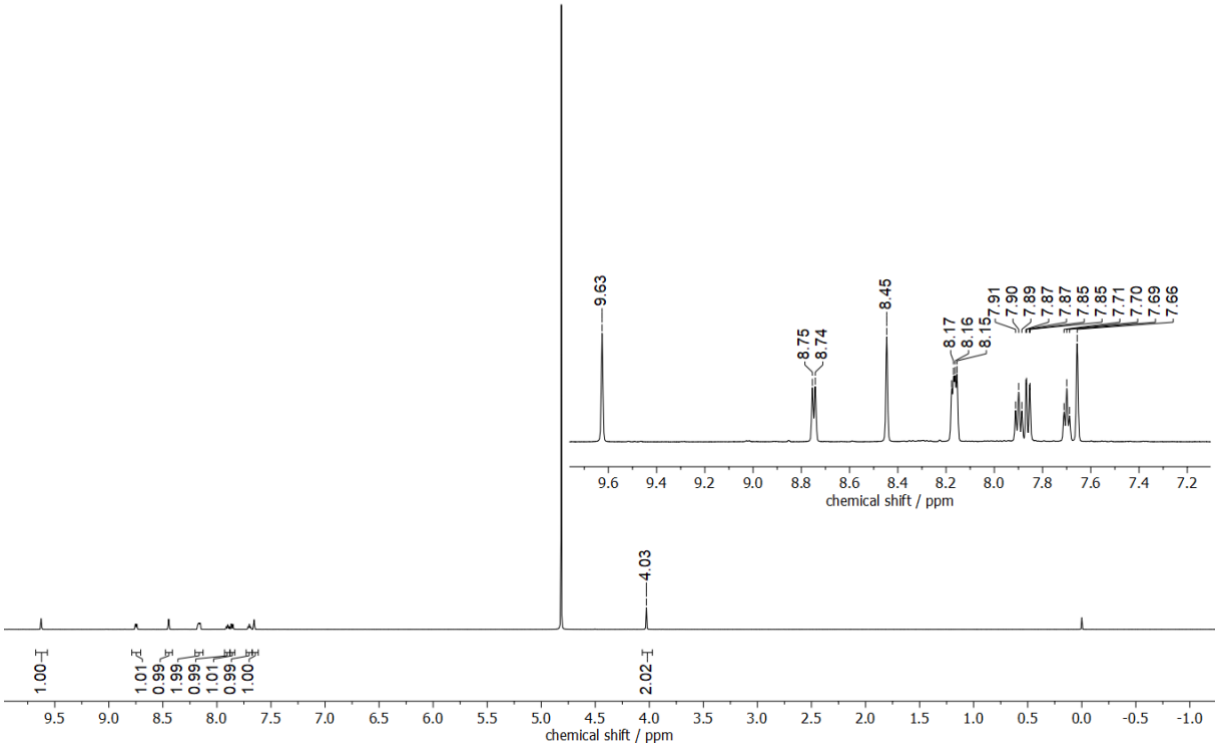

Figure S44. ^{1}H-NMR spectrum (600 MHz, D_2O, 25 °C) of **1**.

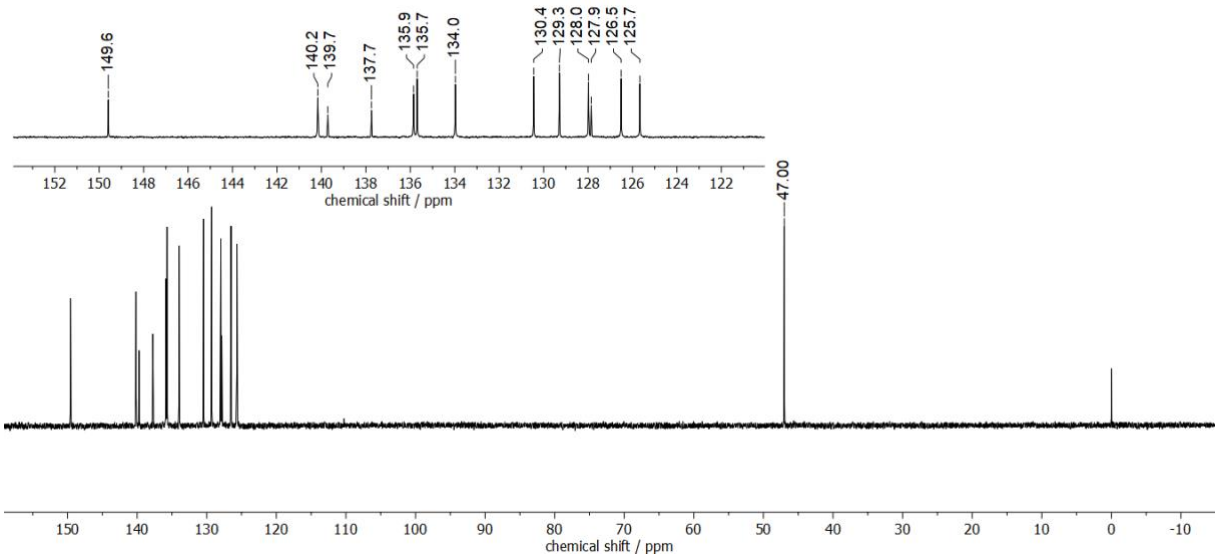

Figure S45. ^{13}C-NMR spectrum (150 MHz, D_2O, 25 °C) of **1**.

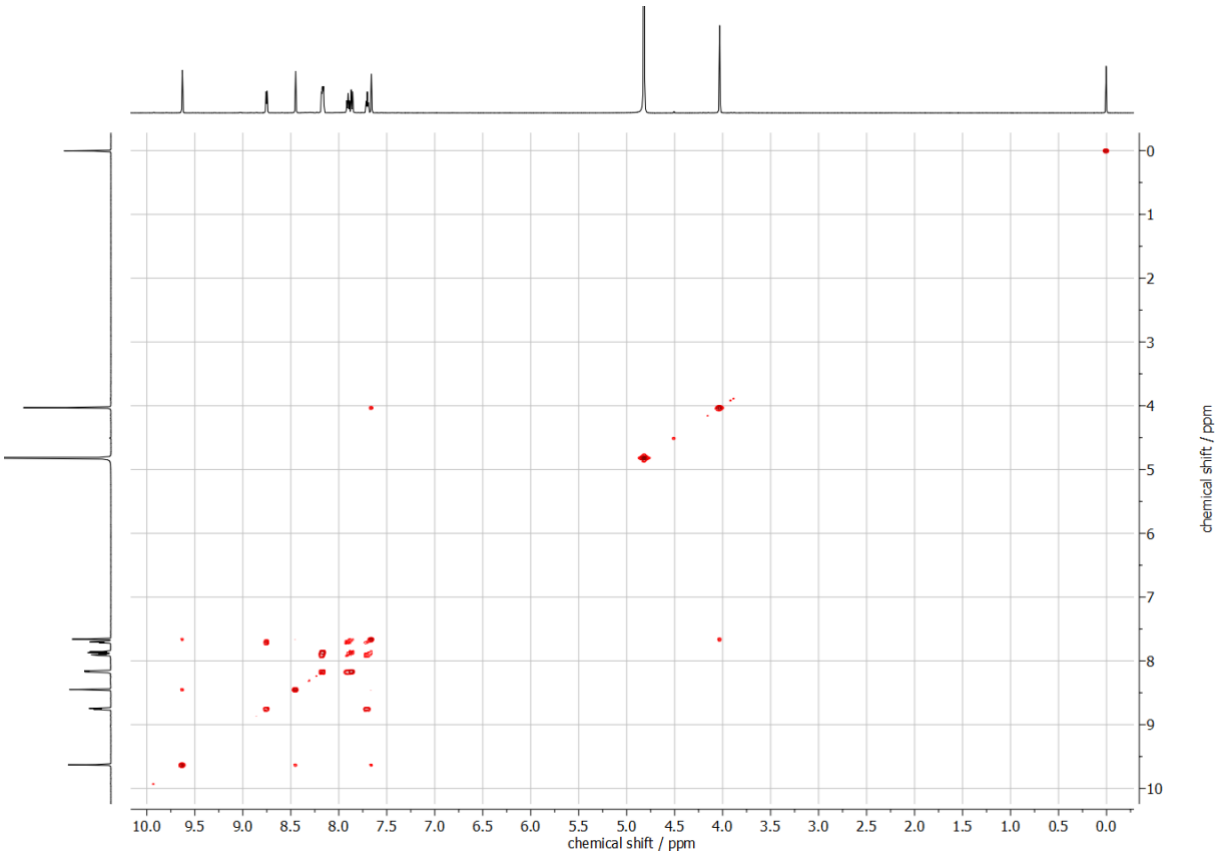

Figure S46. HH-COSY (600 MHz, D_2O, 25 °C) of **1**.

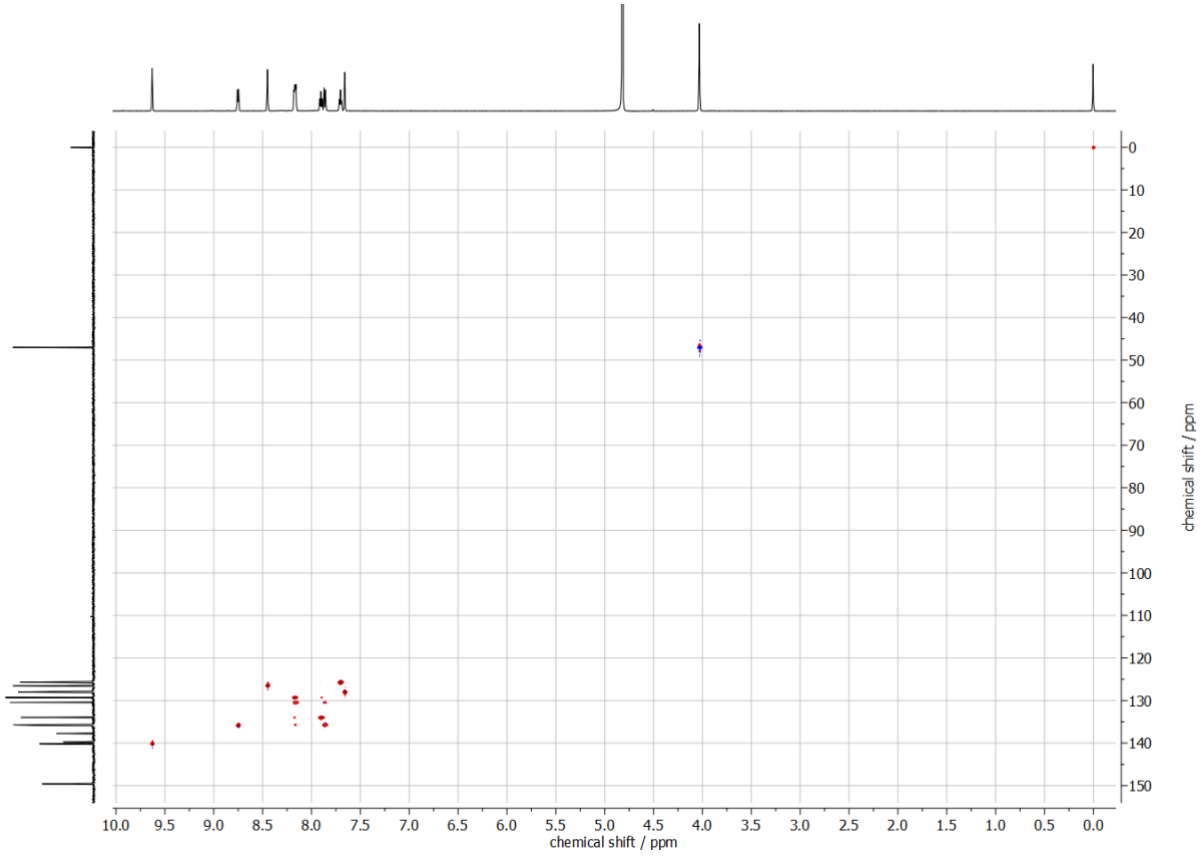

Figure S47. HSQC spectrum (600 MHz, D_2O, 25 °C) of **1**.

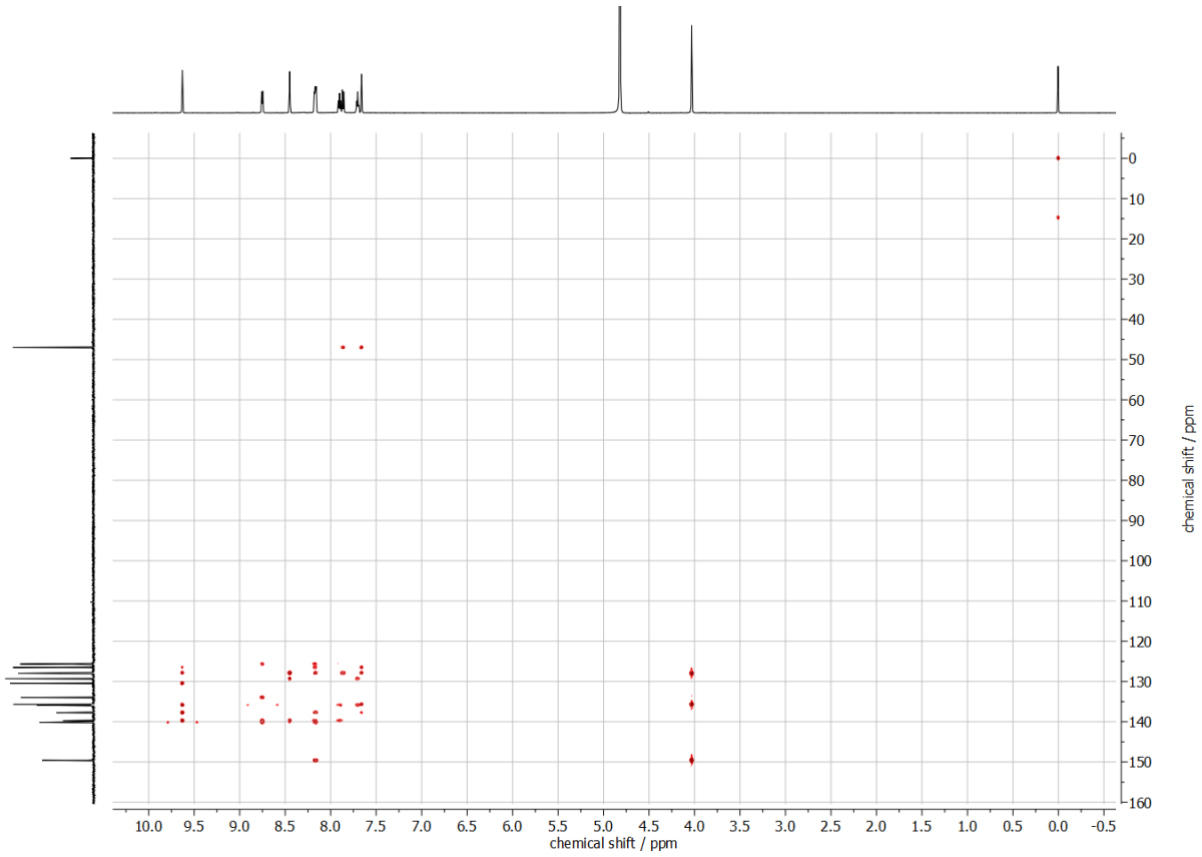

Figure S48. HMBC spectrum (600 MHz, D_2O, 25 °C) of **1**.

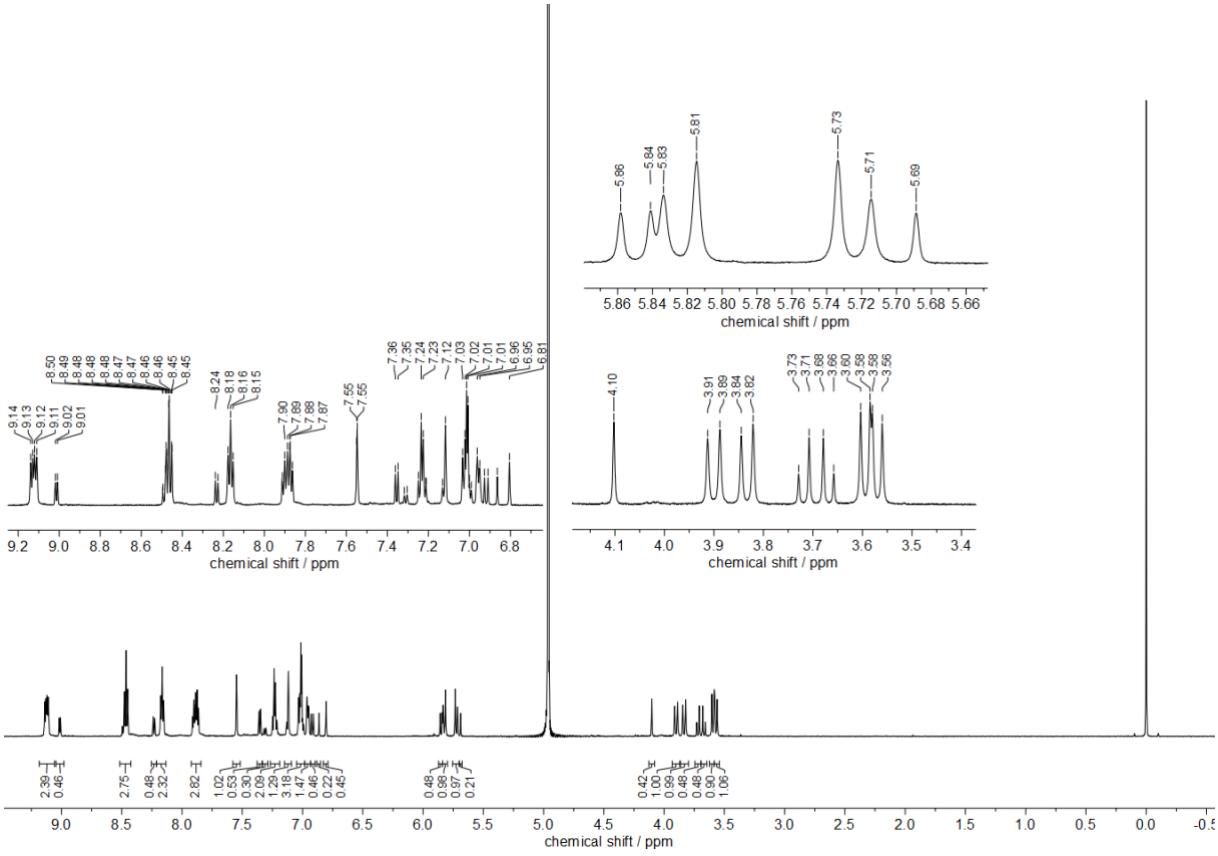

Figure S49. ^{1}H-NMR spectrum (600 MHz, D_2O, 10 °C) of the photoproducts of **1**.

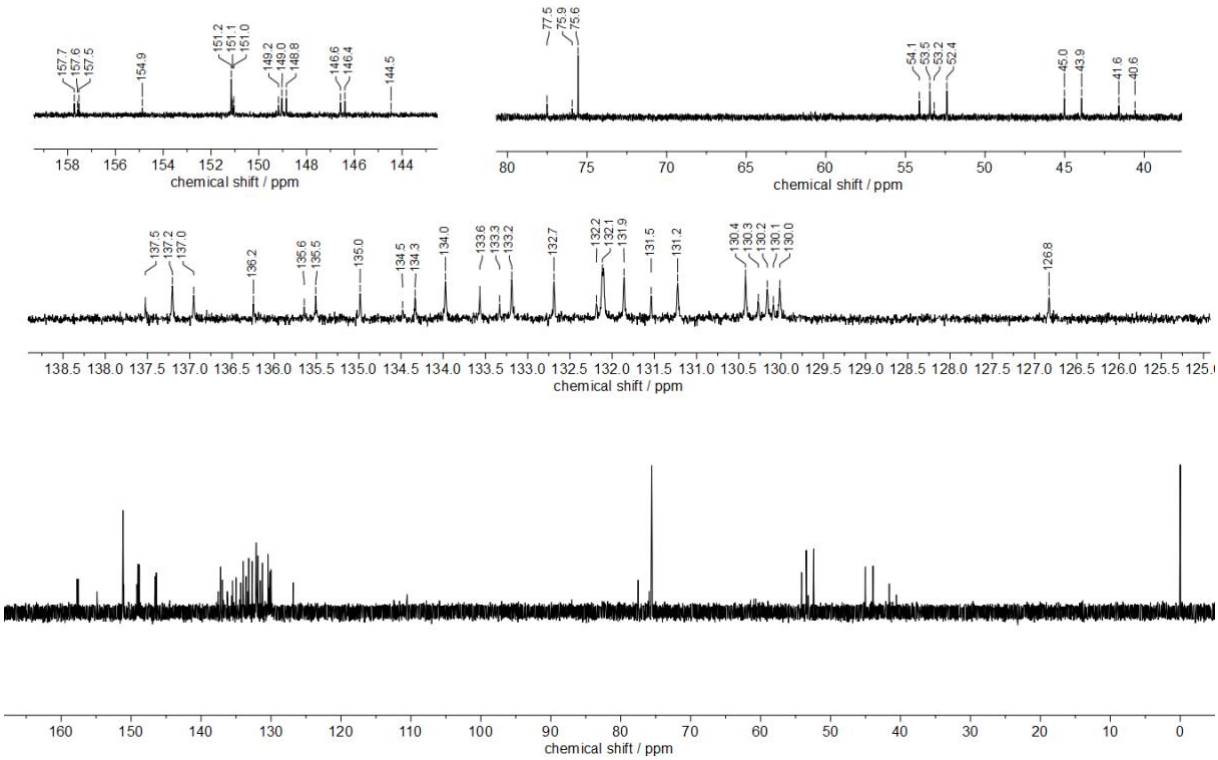

Figure S50. ^{13}C-NMR spectrum (150 MHz, D_2O, 10 °C) of the photoproducts of **1**.

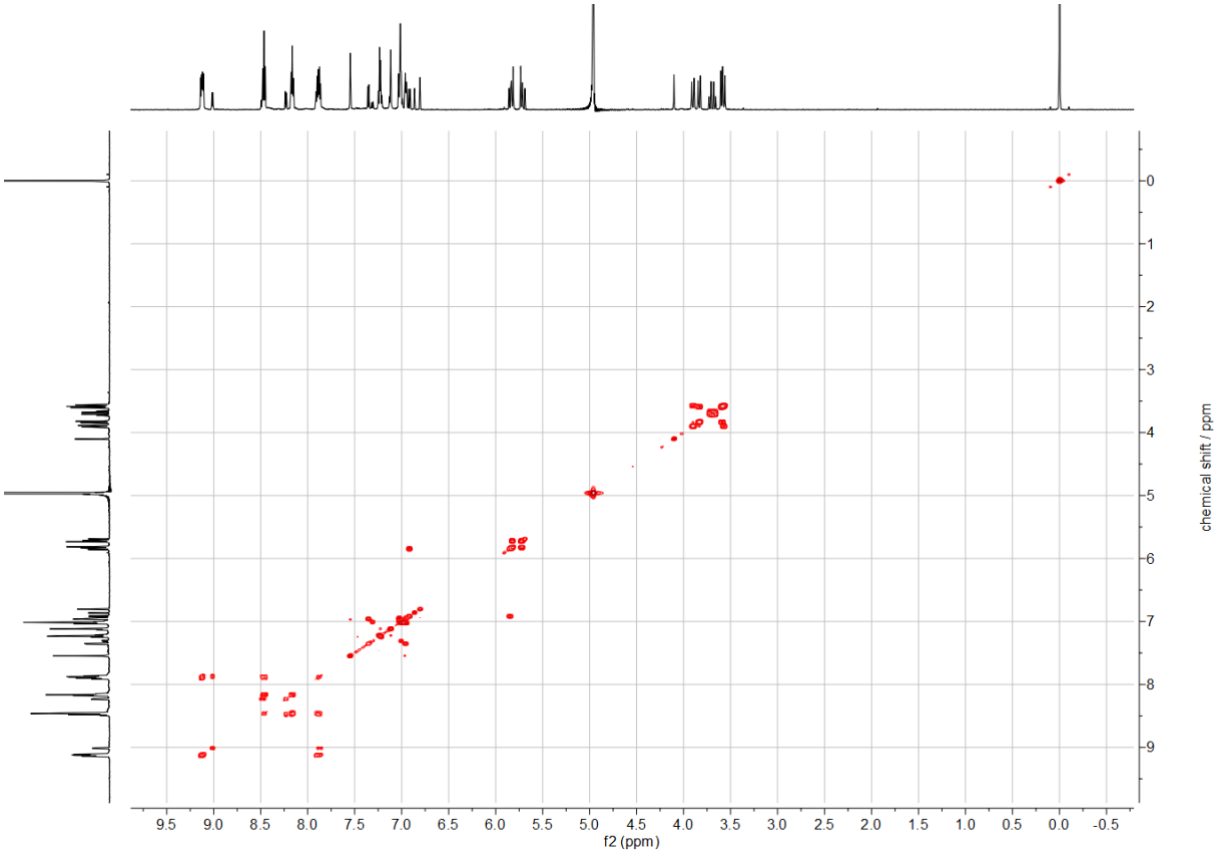

Figure S51. HH-COSY spectrum (600 MHz, D_2O, 10 °C) of the photoproducts of **1**.

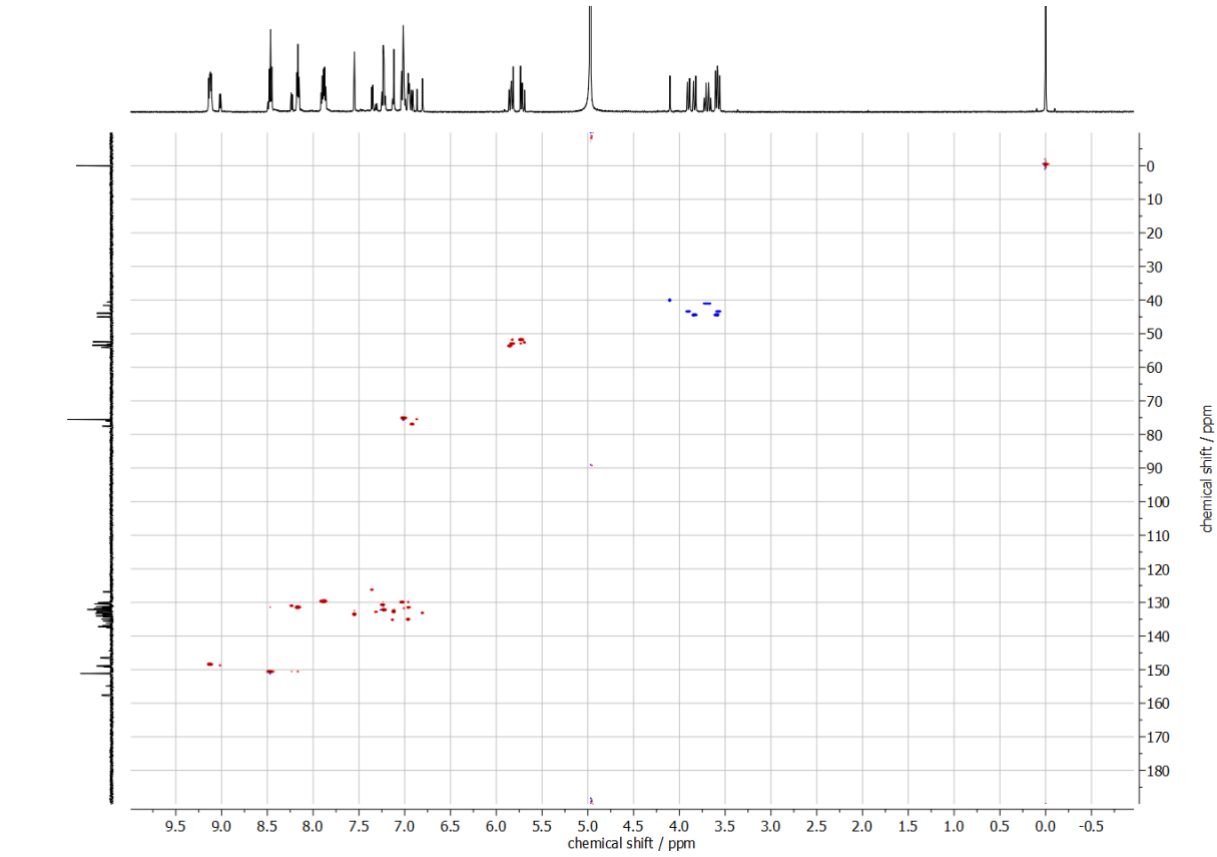

Figure S52. HSQC spectrum (600 MHz, D_2O, 10 °C) of the photoproducts of **1**.

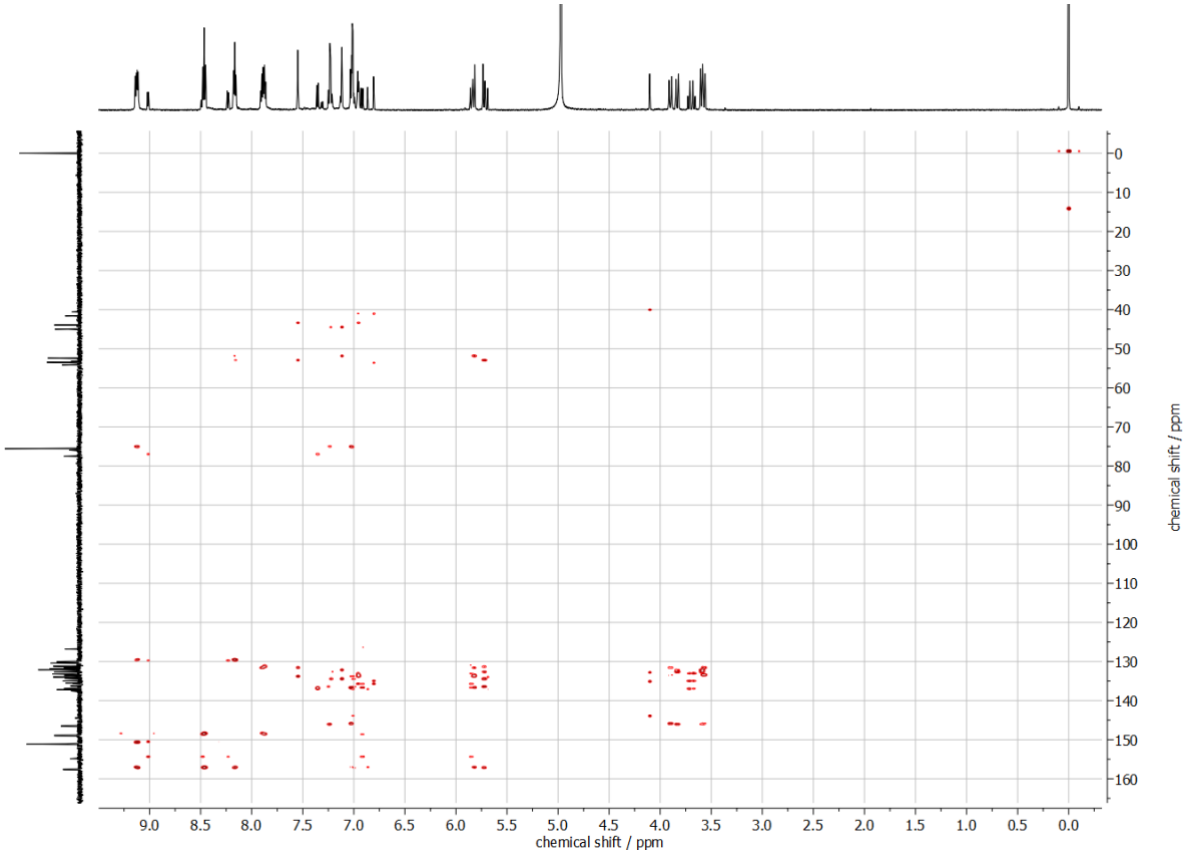

Figure S53. HMBC spectrum (600 MHz, D_2O, 10 °C) of the photoproducts of **1**.

8. References

[1] D. Monchaud, C. Allain, and M. -P. Teulade-Fichou, *Bioorg. Med. Chem. Lett.* 2006, **16**, 4842.
[2] T. Šmidlehner, I. Piantanida, and G. Pescitelli, *Beilstein. J. Org. Chem.*, 2018, **14**, 84.
[3] F. H. Stootman, D. M. Fisher, A. Rodger, and J. R. Aldrich-Wright, *Analyst*, 2006, **131**, 1145.